UNIVERSITY OF CALIFORNIA, SAN DIEGO

Three-dimensional Cardiac Microtissues in a Microfluidic Device: Heart-on-a-chip

A thesis submitted in partial satisfaction of the
requirement for the degree Master of Science

in

Bioengineering

by

Ivneet Singh Bhullar

Committee in charge:
Professor Shyni Varghese, Chair
Professor Andrew McCulloch
Professor Mark Mercola

2015

The Thesis of Ivneet Singh Bhullar is approved and it is acceptable in quality and form for publication on microfilm and electronically:

Chair

University of California, San Diego

2015

TABLE OF CONTENTS

LIST OF FIGURES AND TABLES

ACKNOWLEDGEMENTS

As always, the majority of the credit for my accomplishments goes to my parents and younger brother. Without this close-knit support system, I would not have these achievements for you to be proud of. Thank you Dad for teaching me that castles must be built in air before they can materialize and thank you Mom for instilling within me the value of hard work to enable me to achieve these dreams. Thank you Jorjit for continuing to teach me so much each day even with the 2-year age difference that feels shorter and shorter as the years go by.

Shyni, thank you for your constant guidance, patience and, when necessary, criticisms, without which these 2 years could not have been as fruitful as they were. Your genuine interest and support of my goals since day one encouraged me to be my best and inspired me to develop a work ethic that I know will take me far in life, even if it can never come close to matching yours.

Professors Andrew McCulloch and Mark Mercola, thank you for serving as members of my thesis committee. Without your scientific guidance and critique of this work, its impact would be significantly less.

Aereas and Lynn, without your efforts, this work would not have been possible. Thanks Aereas for applying your scientific expertise and patience in mentoring this study. Thanks Lynn for sharing your experimental expertise to ensure the success of this work.

Gaurav, thanks for everything in lab and beyond. I'm glad we continued this journey that began at UCLA to become more like brothers over these past two years. I have no doubt you will go on to achieve great things in this lab and afterwards.

To the Device and Cell Mechanics Group, the extent of support and collaboration within this group is undoubtedly rare. Thank you Aereas, Han, Shruti, Gaurav, Lynn, and Nailah for keeping each day interesting and making the dark cave of research a little brighter through your comic relief these past 2 years.

Chapters 1, 3, 4 and 5, in part, are currently being prepared for submission for publication of the material. Bhullar, Ivneet S; Aung, Aereas; Theprungsirikul, Jomkuan; Davey, Shruti K; Lim, Han L; Chiu, Yu-Jui; Lo, Yu-Hwa; McCulloch, Andrew; Varghese, Shyni. The dissertation/thesis author was the primary investigator and author of this material.

ABSTRACT OF THE THESIS

Three-dimensional Cardiac Microtissues in a Microfluidic Device: Heart-on-a-chip

by

Ivneet Singh Bhullar

Master of Science in Bioengineering

University of California, San Diego, 2015

Professor Shyni Varghese, Chair

We present the development of three-dimensional cardiac tissues within a microfluidic device with the ability to quantify real-time contractile force measurements *in situ*. Using a three-dimensional (3D) patterning technology that allows for the precise spatial distribution of cells within the device, we created an array of 3D cardiac microtissues from neonatal mouse cardiomyocytes. We integrated the 3D micropatterning technology with microfluidics to achieve perfused cell-laden structures. The cells were encapsulated within a degradable gelatin methacrylate structure, which was sandwiched

between polyacrylamide hydrogels. The polyacrylamide hydrogels were used as "force sensors" to acquire the real-time contractile forces generated by the cardiac cells. We further validated the engineered cardiac microfluidic system's cardiac-specific response to drugs by exposing it to epinephrine, an adrenergic neurotransmitter known to increase the magnitude and frequency of cardiac contractions. Such cost-effective and easy-to-adapt systems with real-time functional readout could be attractive technological platforms for drug discovery and development.

Chapter 1: INTRODUCTION

Development of three-dimensional (3D) cell culture has not only advanced regenerative medicine but also led to the development of physiologically relevant model systems to understand the dependency of cells on the microenvironment for different cellular functions leading to tissue formation. Engineered 3D tissues also offer an invaluable technological platform for drug and small molecule discovery and development. Such systems could provide more physiologically relevant models than currently available monolayer cultures.[1-9] Development of micro-tissues could also circumvent the limitations associated with pharmaceutical testing in animals. While animal models provide an *in vivo* environment with systemic readouts, drug testing in animals is time consuming, costly, and the acquired results can be unreliable due to the innate differences across species.[10,11] Furthermore, form an ethics perspective, development of physiologically relevant *in vitro* platforms could reduce the dependency on animal usage for drug discovery and development. The need for cost-effective and efficient *in vitro* platforms to improve the drug development process has led to the exploration of new technological platforms involving engineered tissue mimics.

One of the organs that have been studied extensively is the heart. Over the past decade, many 3D *in vitro* models for cardiac drug screening have been developed using neonatal cells or human stem cell-derived cardiomyocytes.[3,12-17] Microtissues in these static cultures are able to respond to the changes in environmental cues after electrical and pharmaceutical stimulation.[16,17] While these static cultures have been shown to be effective, it is attractive to integrate perfusion with engineered tissues to improve transport and diffusion of nutrients. Integration of such perfusion can be achieved by

combining the microfabrication of engineered tissues with microfluidics. This also facilitates incorporation of tissue-specific biochemical gradients and dynamic mechanical cues within the system. These systems could also be designed to provide real-time read outs. Such technological platforms, widely known as organ-on-chips, have been developed extensively in recent years.[18,19]

Specifically for cardiac applications, microfluidic heart-on-chip devices have emerged as one of the methods to achieve *in vitro* cardiac models that also allow for the monitoring of drug activity in real-time within dynamic, perfusion-based culture that better mimics the circulatory system.[20-25] Parker and colleagues have combined their muscular thin film (MTF) technology with microfluidics to create a heart-on-chip.[21] One of the key features of functional cardiac tissues is their ability to beat. Hence, measuring the contractile stresses generated by the microtissues could be used as readout to examine the response of the tissue against various environmental cues, including small molecule drugs. To this end, Parker and colleagues have used MTF technology to quantify the contractile stresses generated by cardiac cells. This system has further been extended to study pathophysiological changes in cardiac tissues.[26,27] Nevertheless, this system consists of 2D cardiomyocyte monolayers and thus loses the *in vivo* relevance of other 3D tissue models. In a recent study by Healy and colleagues, a microfluidic model was developed that incorporated iPSC-derived 3D cardiac tissues within a microfluidic system and demonstrated its applications in drug screening.[20] The researchers have used calcium signaling and beating frequency as functional readouts. However, the cell pellet method for forming 3D cardiac tissue used in this system does not allow for precise spatial control of cell seeding within the tissue, while also depriving the tissues of an

ECM-mimicking material as a scaffold to facilitate cell-ECM interactions. Further, the device does not provide for the measurement of contractile forces in real-time, an integral indicator of healthy cardiac function and drug responsiveness.

Here in this paper, we describe the development of a novel microfluidic device capable of quantifying contractile forces *in situ*. This device involves a vertical tri-layer hydrogel system where a 3D cell-laden structure is sandwiched between two acellular structures and is perfused with microchannels**.** This was achieved by integrating 3D patterning technology, to encapsulate cells in a spatially controlled manner, along with a far-field concept to measure contractile forces generated by the cardiac structures. In this proof-of-concept, we have used neonatal mouse cardiomyocytes as a cell source and tested the cardiac-specific response of the system to epinephrine. Thus, this system capitalizes on the physiological relevance of 3D structures and perfusion-based microfluidic systems while introducing a novel technique to monitor cardiac functionality by measuring contractile forces.

Chapters 1, 3, 4 and 5, in part, are currently being prepared for submission for publication of the material. Bhullar, Ivneet S; Aung, Aereas; Theprungsirikul, Jomkuan; Davey, Shruti K; Lim, Han L; Chiu, Yu-Jui; Lo, Yu-Hwa; McCulloch, Andrew; Varghese, Shyni. The dissertation/thesis author was the primary investigator and author of this material.

Chapter 2: LITERATURE REVIEW

2.1) Tissue Engineering trends

Although the regeneration of human tissues and organs to preserve and prolong life has always been a topic of dream and science fiction, it was not until the last three decades that the field of tissue engineering really took off to make such myths a reality. Since the coining of the term "tissue engineering" in 1987, researchers have worked to continuously modify its definition by introducing innovative studies hinged on applying engineering principles to living systems. Many of the advancements in this field have focused on the use of stem cells for the remodeling or regeneration of tissues to restore function to injured or defected human tissues or organs, falling under the specific field of regenerative medicine. Most would agree the major developments in tissue engineering began with tissue engineered skin studies and products in the late 1970s and early 1980s[28-31], which were later expanded to collagen-based skin therapies[32,33], and followed eventually by the first cell transplantation within synthetic biodegradable polymers by the end of the decade.[34] With the discovery of human embryonic stem cells in 1998, stem cells emerged as a unique source for tissue engineering applications. Further progress in this field was spurred by the advent of unique progenitor cell sources, with the discovery and development of induced pluripotent stem cells (iPSCs) in 2006 proving to be perhaps the most impactful development in the stem cell area.[35] This breakthrough has facilitated the rapid growth of tissue engineering, with stem cell based therapies and patient-specific drug discovery and medicine among the most promising outcomes of the use of such pluripotent cell sources.

While the initial efforts in tissue engineering focused on repairing and replacing compromised tissue and organs, recent goals have shifted to the development of model systems recapitulating physiological conditions. Such models can be used for studying developmental processes, perturbing diseased states, as well as serving as drug and small molecule screening platforms. Such model systems have experienced significant progress in recent years as the field has shifted from two-dimensional (2D) to three-dimensional (3D) *in vitro* models in a dish, and from static to dynamic flow culture systems.

2.2) Two-dimensional vs. three-dimensional *in vitro* culture systems

Until recently, the majority of advances in cell and tissue engineering have relied on the assumption that 2D monolayer cell cultures accurately represent complex *in vivo* physiology. However, it is well known that flat, 2D polystyrene or glass surfaces do not recapitulate the full extent of extracellular matrix (ECM) interactions as seen *in vivo*. Such 2D monolayer environments are known to display significant differences from complex biological and biochemical mechanisms seen in the physiological environment, such as receptor expression, transcriptional expression, cellular migration and apoptosis. Such differences can be attributed to the failure of 2D monolayer systems to recapitulate the biochemical and mechanical cues that govern cell-cell and cell-ECM interactions.[2] Recent studies in tumor biology, cell adhesion and migration, and cardiac contractility further highlight the differences seen between 2D and 3D culture systems, with the latter showing increased levels of complexity. Briefly, it has been shown that 2D culture fails to reproduce the bidirectional cross-modulation of receptors that is seen in 3D cultures of human breast tumor cells.[4] Additionally, studies indicate that fibroblasts cultured in 3D

matrices have a more physiologically relevant shape, motility and functionality than those on a 2D substrate, with those in 3D resembling *in vivo* adhesion structure and localization more closely.[7-9] The unique fibroblast adhesions and motility seen in 3D cultures facilitate the invasive functions of fibroblasts as seen *in vivo*.[9] Further, it has been shown that cardiac cells in a 3D environment display significantly higher contractile force as well as stronger cell-cell interactions when compared to cardiac cells seeded on 2D surfaces.[3]

Such studies highlighting the increased physiological relevance of 3D cultures compared to 2D cultures caused a push for more systems that could better reproduce *in vivo* characteristics. To this end, tissue engineering has been used as a tool to produce 3D models by encapsulating cells within biomimetic scaffolds. In addition to this approach, current *in vitro* 3D culture models include organotypic explant cultures, cellular spheroids, and microcarrier cultures, which are highlighted in Figure 1 (adapted from reference [36]). Organotypic explant models are used primarily where data is mandated from cells embedded within their native tissue.[2] Cellular spheroid models arise from the tendency of adherent cells to aggregate and have recently gained popularity for use in tumor growth and cancer metastatic studies.[2] Furthermore, although initially developed for use in vaccine production, microcarriers have recently been further developed with Rotating Wall Vessel bioreactors[37] to produce biomimetic structures of intestine,[38-40] lung,[41] and bladder.[42] Thus, various 3D culture methods have been used to study a multitude of organs and tissues in an *in vitro* environment that allows for cells to interact in all three dimensions.

2.3) Cardiac physiological considerations for *in vitro* models

The heart is one such organ that has been studied due to the prominent impact of congestive heart failure. Recent numbers from the California Institute of Regenerative Medicine indicate that heart disease causes one third of all deaths in the United States, with an estimated 4.8 million Americans suffering from congestive heart failure. Further, approximately one third of pharmaceutical failures are due to safety issues arising from cardiotoxicity.[20] Therefore, physiologically relevant *in vitro* cardiac models can be used to gain valuable insight into the pathophysiology of specific disease states as well as screening promising pharmacological agents for cardiotoxicity.

However, such systems must recapitulate *in vivo* environments by mimicking as many aspects of the native cardiac environment as possible. The adult heart is known to balance a composition of many cells, including cardiomyocytes, cardiac fibroblasts, vascular smooth muscle cells and endothelial cells, within an organized ECM.[43] Although the majority of the cardiac tissue volume consists of cardiomyocytes, they only make up 30% of the cellular composition, with the majority of the remaining cells being cardiac fibroblasts.[44] Endothelial and vascular smooth muscle cells are restricted to the vasculature, and each cardiomyocyte is estimated to be connected to one or more cardiac fibroblasts by cell-cell connections facilitated by connexins and cadherins.[45] Cardiomyocytes consist of aligned sarcomeres, the functional unit of cardiac muscle cells, that give cardiac muscle its striated appearance. Although cardiomyocytes are the cells that induce the contractions of the heart, cardiac fibroblasts are essential to the structural, biochemical, mechanical and electrical properties of the heart.[46] In addition to contributing significantly to the synthesis of ECM, cardiac fibroblasts have been shown

to respond to various cues, including electrical, mechanical and chemical stimuli.[45] Furthermore, cardiac fibroblasts have also been shown to secrete growth factors and cytokines essential for cardiac tissue function.[47] Finally, although cardiac fibroblasts themselves are not capable of spontaneous contraction, they have been shown to facilitate electrical interactions between distant cardiomyocytes, contributing to coordinated contraction in the heart.[45,46] Thus, multiple cell types play important roles in native cardiac tissue and they must all be considered for ideal *in vitro* cardiac models.

2.4) 3D *in vitro* cardiac models

Recently, *in vitro* 3D cardiac models have gained interest with various studies focused on the development of such systems.[3,12-16] Researchers from the University of Pennsylvania recently created 3D cardiac microtissues by embedding neonatal rat cardiomyocytes within collagen matrices located within arrays of wells on the surface of a polydimethylsiloxane (PDMS) substrate.[12] Two cantilevers were incorporated to ensure linear tissue alignment and contraction as well as to measure the forces generated by these cardiomyocytes by observing the displacement of fluorescent microbeads at the top of the cantilevers. A different approach was taken by Kim et. al. to create a model with both 2D and 3D cardiomyocyte culture systems.[3] Cells were seeded onto individual cantilevers consisting of flat and grooved PDMS surfaces, with the former representing a 2D culture surface and the latter designed to mimic the *in vivo* 3D environment. Interestingly, this system showed that cardiomyocytes cultured on the grooved surfaces showed a higher degree of actin organization as well as 65-85% higher contractile force. Additionally, a study from the University of Michigan documented the use of a culturing

technique in which a 2D monolayer of cardiomyocytes seeded on a laminin substrate spontaneously formed a 3D cylindrical structure that maintains cell-cell interactions as well as coordinated contraction.[13] In this unique study, 3D cardiac structures were produced without the use of a scaffold, attributing the mechanical integrity of the construct primarily to cell-cell interactions. In another example of *in vitro* 3D cardiac culture, a team of German scientists was able to determine the tension caused by the contraction of cardiac cells seeded both as a monolayer and within a flexible, 3D collagen scaffold.[14] Their unique system allows for the forces of contraction to be measured as oscillating differences in pressure as the cardiac cell layers and constructs contract. Also, the ability of this system to apply a controllable pressure to the cells opens the door for the modeling of certain cardiac disease states such as heart failure caused by hypertension. Furthermore, a study by Khademhosseini et. al. details a procedure in which a microfluidic patterning technique is used to produce 3D cardiac structures on a glass surface *in vitro*. After the patterning of hyaluronic acid (HA) on a glass surface, seeded neonatal rat cardiomyocytes preferentially bind to the glass surface and the interface between the glass surface and patterned HA. The HA patterns function as templates for the formation of 3D cardiac structures as 2D cells detach after 3 days to form constructs that exhibit coordinated contraction.

These examples of 3D *in vitro* cardiac cultures all show the rapid growth such models have experienced in just the past decade with the use of neonatal rat cardiomyocytes as proof-of-concept cell sources in most cases. However, the study by Thavandiran et. al. highlights the recent strides that have been made in incorporating pluripotent stem cell (hPSC)-derived cardiac cells to form 3D cardiac microtissues *in*

vitro. In this study, the authors used a combination of computational modeling and experimental methods to establish design criteria, consisting of tunable electromechanical stimulation and cell composition, for creating 3D hPSC-derived cardiac microtissues. First, finite element models were used to generate two potential microtissue geometries, with one designed to simulate biaxial intratissue tension forces (BITFs) and the other to simulate uniaxial intratissue tension forces (UNITFs). The objective was to discern the relationship between stress distributions and regions of sarcomere alignment within the microtissue, which is an indicator of healthy cardiac tissue. This model predicted regions of stress and sarcomere alignment only in the border areas of microtissues with BITFs. On the other hand, it predicted stress distributions and sarcomere alignment along the longitudinal axis of microtissues with UNITFs. Sarcomere alignment along the predicted stress regions was confirmed for both models with sarcomeric α-actinin immunostaining. Thus, the authors concluded that microtissues under UNITF promoted the formation of aligned and highly organized sarcomeres and additional proteins necessary for contraction, better mimicking physiological cardiac muscle fibers.

However, variability was seen in tissue physiology due to uncontrolled cell composition. Thus, the authors seeded microtissues with varying ratios (100:0, 75:25, 50:50, 25:75) of NKX2-5+ cardiomyocytes to CD90+ nonmyocytes, in which the latter were considered to be primarily fibroblasts. The authors saw similar remodeling in all conditions except the 100:0 case in which the collagen gel matrix compaction was limited most likely due to the lack of fibroblast-induced remodeling. Additionally, with increasing ratio of fibroblasts, more compact and integrated tissue morphologies were seen due to increased levels of tension. As a result of this, the tissues with ratios of 50:50

and 25:75 did not survive to day 7 due to fibrosis caused by high levels of tension. On day 7, the authors reported seeing spontaneous contractions in tissues of ratios 100:0 and 75:25; however, of these, only the 75:25 tissue sample displayed synchronous contractions and a homogenous spatial distribution of cardiomyocytes and fibroblasts, as shown by the fluorescence of NKX2-5+ cells along with staining for vimentin, a fibroblast marker. After further confirming these results by assessing cardiac-specific gene expression, the authors concluded that a 3D microenvironment under uniaxial mechanical stress and a strategically determined cell fraction of cardiomyocytes to fibroblasts are both critical design criteria for creating physiologically relevant, *in vitro* cardiac tissues. Furthermore, microtissues created under these conditions were used for functional assays to show physiologically appropriate responses of the microtissues to drugs of known cardiac effects. Epinephrine (0.1 μg/mL), an adrenergic neurotransmitter, increased the contraction frequency, lidocaine (2.0 μg/mL), an antiarrhythmic drug, decreased the contraction frequency, and verapamil (0.25 μg/mL), an L-type calcium channel blocker, reduced the amplitude of calcium waves. Finally, the group was also able to induce tachycardia in the microtissues, showing the utility of this method to produce *in vitro* disease models using hPSC-derived cardiomyocytes.

2.5) Limitations of static culture conditions

Thus, researchers have clearly made significant progress towards creating 3D cardiac *in vitro* models that can serve as better predictors of the *in vivo* cardiac environment. However, there is one significant physiological aspect that these culture systems have not been able to replicate: the circulatory system. Static cell culture systems

rely on simple diffusion to facilitate the exchange of nutrients and waste between cells and the surrounding culture medium. This method works well for 2D monolayer systems in which all cells are afforded direct and sufficient contact with the medium, allowing the medium to be sufficient for an extended period of time until it must be replenished to remove waste and provide fresh nutrients. However, with 3D culture systems simple diffusion proves to be inadequate as the dimensions of 3D structures increase, further removing cells from direct contact with medium. Thus, the dimensions of 3D *in vitro* models are limited by static cell culture conditions. Physiologically, this problem is combatted by the vast circulatory system, with extensive vasculature providing nutrients to and transporting waste from cells.

2.6) Organ-on-chip systems

To recapitulate the benefits of the circulatory system, dynamic culture techniques have recently gained interest due to their ability to provide a continuously replenished supply of nutrients through a combination of convective and diffusive transport. Studies on many different types of tissue constructs, including cardiac tissues *in vitro*, have shown the increased value of dynamic culture over static systems.[48-53] Particularly, microfluidic systems have become increasingly popular due to their ability to provide tunable fluid flow that recapitulates the effects of native microvasculature, providing convective transport of fresh nutrients, soluble cues and waste. Microfluidics is a field at the intersection of engineering and biology that involves the flow of small amounts of fluid volume through microfabricated channels. Tuning fluid flows through microfluidic devices that house 3D tissue structures allows scientists to manipulate spatiotemporal

gradients of nutrients and soluble cues to match physiological levels, thus creating 3D microenvironments that mimic *in vivo* environments better than traditional static culture of 2D models. This technology has been employed to create 3D *in vitro* microfluidic models of various systems, including heart, blood vessels, bone, bone marrow, brain, blood-brain barrier, breast, cancer, eye, gut, kidney, liver, lung, muscle, nerve and skin (Table 1).

Table 1: Summary of microfluidic organ-on-chip systems

Organ	Culture Type	Refs.
Heart	2D, 3D	20-25,54,55
Blood vessels	2D, 3D	56-58
Bone/Bone Marrow	2D, 3D	59-63
Brain/Blood-brain barrier	2D	64-69
Breast	2D, 3D	70,71
Cancer	3D	72
Eye	3D	73
Gut	2D	74-79
Kidney	2D	80-84
Liver	2D, 3D	85-99
Lung	2D, 3D	95,100-104
Muscle	2D, 3D	105
Nerve	2D	106-110
Skin	2D	111

2.7) Heart-on-chip systems

Heart-on-chip platforms have made significant progress in the past decade. In 2006, researchers studied the ionic and metabolic fluxes of single cardiomyocytes by integrating five electrodes within a microfluidic system.[24] They were able to use these

electrodes to stimulate the cell while measuring its lactate production and contractility as well as pH and calcium levels. Although a significant step towards building devices to recapitulate the *in vivo* cardiac microenvironment, information obtained from this device was only applicable to individual cardiac cells. Moving towards more physiologically relevant systems, scientists began incorporating 2D cardiac cell cultures within microfluidic devices. Researchers developed a microfluidic cell culture model that allowed for mechanical loading seen *in vivo* that typical *in vitro* models could not provide without the use of microfluidics.[25] By employing fluid induced loading, they were able to reproduce various hemodynamic loading conditions associated with the healthy and failing native heart, providing an *in vitro* model to study disease states such as hypertension, hypotension, tachycardia and bradycardia. A later study also used a microfluidic heart-on-chip technology to induce ischemia/reperfusion injury in a 2D cardiac model, further validating the utility of such devices for reproducing diseased *in vivo* environments.[22]

Muscular thin film (MTF) technology has emerged as a convenient tool in assembling *in vitro* cardiac models from which useful information can be drawn about cardiac drug response and disease models. MTF technology allows for the measurement of important cardiac functional elements such as contractility, tissue structure and electrophysiological properties. This model has been combined with microfluidic technology by Agarwal et. al. to produce a heart-on-chip platform in which arrays of thin film cantilevers composed of soft elastomers are seeded with a monolayer of cardiomyocytes. They were able to develop a semi-automatic fabrication system (Fig. 2A) that generates these MTFs in a reproducible fashion while also increasing the

throughput of using such technology. These cell-seeded cantilevers were housed within a microfluidic device (Fig. 2B) that was designed using fully autoclavable materials and that included a metallic base (for temperature control), transparent top (for taking measurements *in situ*), and embedded electrodes (for stimulation of contraction). Once assembled, the authors proved the utility of this system by collecting contractile data from the system *in situ*. As the cardiomyocytes seeded on the MTFs contract, the cantilevers extend in the third dimension, allowing for characterization of the contractile forces generated by the cardiac cell monolayers. Using this principle, the authors quantified the stresses generated by the cardiac cells, with an average peak systolic stress that aligned well with values obtained from previous studies involving MTFs static culture. Through immunostaining, the authors also showed monolayer alignment of sarcomeres on the thin films, thus proving the potential of this device to provide structural and functional readout. Further, the changes in contractility of the MTFs in response to various concentrations of isoproterenol were studied to validate the ability of the device to mimic the *in vivo* response to drugs of known cardiac effect. As expected, isoproterenol induced cardiac excitation effects in the MTFs, as seen through the general increase in contractile stress with increased dosage of the pharmacological agent. Thus, this group was able to develop a high throughput cardiac heart-on-chip model that combines MTF technology with microfluidics while also allowing for functional and structural measurements. Recently, they have also shown the ability of this system to model several cardiac diseased states.[26,27]

However, this system hinges on 2D monolayer cultures of cardiomyocytes that are seeded on thin film cantilevers, thus losing the physiological relevance provided by

3D culture models. Although researchers have combined explanted human cardiac tissue with microfluidics, such samples have been shown to remain viable for only 3.5 hours, limiting the time scale of studies using these 3D heart-on-chip devices.[54,55] However, Mathur et. al. recently published a study detailing the design, fabrication and utility of a 3D heart-on-chip system for drug screening applications. Their microfluidic system incorporated human cardiac cells, derived from hiPSCs, into 3D tissues that were perfused while allowing for biological, electrophysiological and physiological analysis. In developing this device the researchers focused on three major design criteria to mimic the *in vivo* environment: 1) 3D tissue structure that has multiple layers of alignment of sarcomeres, 2) fluid flow that reproduces the physiological transport properties of microvasculature, and 3) protection of the 3D tissue from shear forces while allowing for diffusive transport from the flow system. To this end, a device was developed that contains a central cell chamber, for the 3D tissue, flanked by two media channels, for the flow of nutrients, with connecting microchannels for diffusive transport (Fig. 3A and B). The dimensions of the media channels (30 – 40 μm) and microchannels (2 μm) were chosen to recapitulate *in vivo* diffusive transport of nutrients through epithelial barriers of the vasculature. Next, to ensure the formation of a 3D cardiac tissue without the use of an ECM scaffold or synthetic matrix, cardiomyocytes were loaded into the central cell chamber of the device at a high density. The high packing density ensured the formation of a 3D cardiac tissue within 24 hours that showed coordinated contraction aligned along the major axis of the tissue after 7 days. Confocal microscopy further confirmed aligned tissue morphology with multiple cell layers. Further, by deriving cardiomyocytes from

hiPSCs genetically engineered to express a specific reporter, they were able to monitor calcium currents arising from tissue contraction using an optical microscope.

Finally, to validate the human-specific cardiac responsiveness of this device to pharmacological agents and drugs with known cardiac effect, the device was perfused separately with isoproterenol (β-adrenergic agonist), E-403 (hERG blocker), Verapamil (multi-ion channel blocker) and Metroprolol (β-adrenergic antagonist). The readout that was used for determining the appropriate effect of these agents was beat rate. Since all four were proven to induce the expected cardiac effect in the 3D tissue, the authors concluded that this 3D heart-on-chip system offers physiologically relevant information for studying human-specific drug responsiveness.

Thus, Mathur et. al. were able to produce a functional 3D heart-on-chip system that shows the significant progress that has been made in these technologies since they were first conceived almost a decade ago. However, the need to further improve the functional readout of such systems still remains. For example, although Mathur et. al. studied the functionality of this tissue with multiple modes of analysis, one of the key functional characteristics of cardiac tissue is the generation of contractile force, which was not quantified in their paper. Many cardiac diseases manifest when cardiac contractility is decreased, inhibiting the heart's ability to effectively pump blood. Relying only on contraction rate as a reliable readout for determining the toxicity and efficacy of pharmacological agents could lead to a misleading conclusion on the drug's effects. A system that can combine the benefits of 3D tissue structure with the ability to monitor the toxicity and efficacy of drugs through real-time force readout in addition to contraction frequency and other modes of analysis would provide an *in vitro* platform from which

meaningful information can be drawn. Such a heart-on-chip system holds great potential for integration into current drug screening protocols.

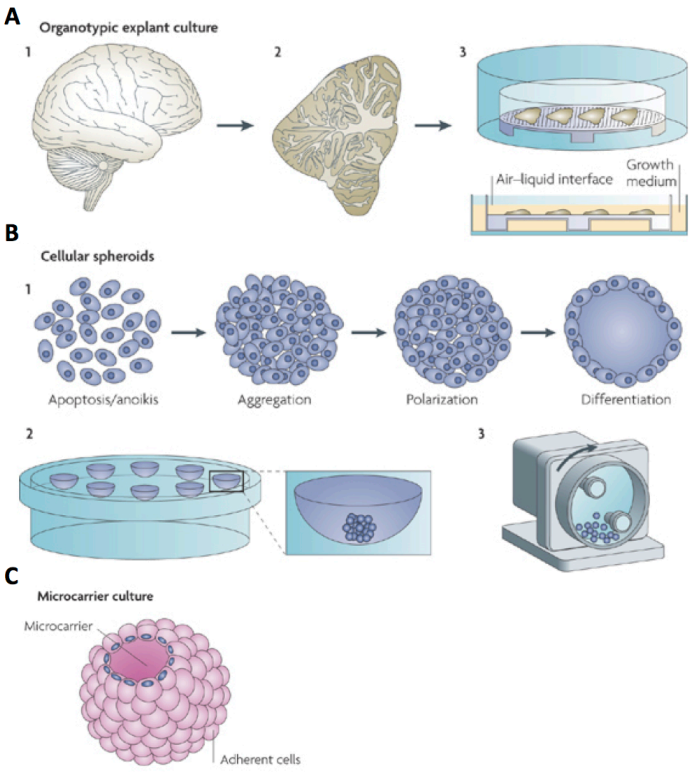

Figure 1: Additional types of 3D *in vitro* culture models. Adapted from reference.[36] In addition to tissue engineered models, 3D culture models include (A) organotypic explant culture, (B) cellular spheroids and (C) microcarrier culture. (A) In organotypic explant culture, dissected organ slices are cultured on porous substrates. (B) Cellular spheroids can be generated through spontaneous aggregation of cells (1) or through culture in a hanging drop (2) or rotating wall vessel (3). (C) 3D matrices made of porous polymers can be used as support to culture adhesive cell lines.

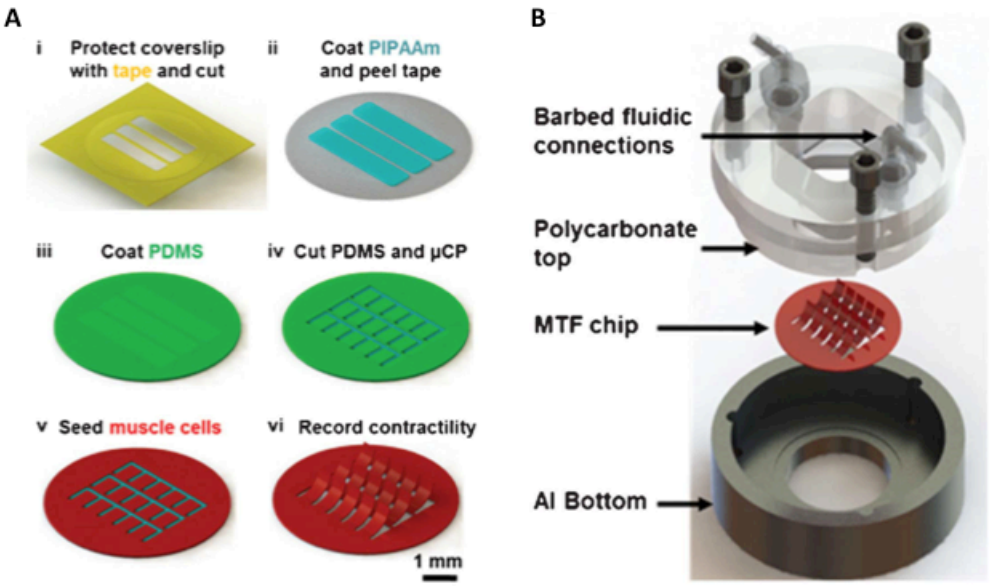

Figure 2: Fabrication of MTFs and incorporation within microfluidic chip. Adapted from reference.[21] (A) Fabrication of MTFs is described where PIPAAm stands for poly(N-isopropylacrylamide), PDMS stands for polydimethylsiloxane and μCP is the process by which precise cuts are made. (B) A blown up schematic is shown for the integration of MTFs in a microfluidic device that allows for imaging.

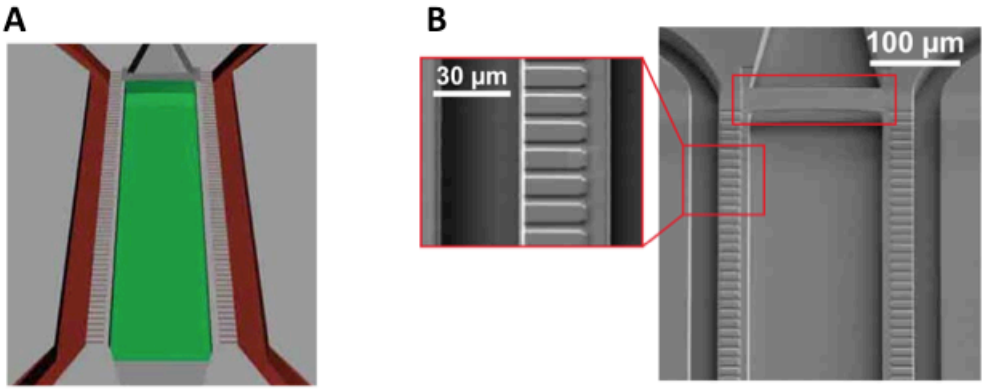

Figure 3: 3D Heart-on-chip system by Mathur, et. al. Adapted from reference.[20] (A) Schematic of heart-on-chip system with cell chamber and fluid channels shown in green and red, respectively. (B) Electron microscope image of system showing cell chamber (100 µm) and zoomed in image of fluid channels (30 µm) along with smaller channels (2 µm) that provide an epithelial cell-like barrier for diffusion.

Chapter 3: MATERIALS AND METHODS

3.1) Fabrication of silicon mold

Firstly, microfluidic channels were photolithographically defined using NR9-1500PY negative photoresist (Futurrex, Frankling, NJ, USA) on 4 inches Si wafer. The Si mold master was etched by using deep reactive ion etching (DRIE) process. In the DRIE process, SF6 gas was flowed at 100sccm during the 11 s of reaction time, followed by a passivation cycle when C4F8 gas was flowed at 80 sccm for 7 s. A 75 μm of etching depth was achieved under the etching rate of about 0.7 μm per cycle. After the DRIE process, the NR9-1500PY photoresist was removed by immersion in acetone for 4 hours before rinsing with methanol, isopropanol, and deionized water. The Si mold was then blown dry by nitrogen gas and silanized by vapor deposition of trichlorosilane (TCI Inc, Portland, OR, USA) to facilitate PDMS demolding.

3.2) Synthesis of Polyacrylamide hydrogels

12mm round glass coverslips and 24x50mm rectangular glass coverslips were first cleaned by treatment with 2.5M NaOH for 20 minutes, and then rinsed with DI water and air-dried. A silane solution was applied for 5 minutes to chemically functionalize the glass, and then the coverslips were once again rinsed and dried. Finally, a 0.75% glutaraldehyde solution was applied for 30 minutes followed by rinse and dry.

PAm hydrogels were synthesized by mixing together 6.25μL of 40% acrylamide solution, 5.625μL of 2% bisacrylamide solution, and 37.25μL of PBS. Fluorescent green beads were added to this 50μL solution at a 1:100 dilution, and 0.6μL of ammonium persulfate (APS) was added from a 10% wt/vol stock solution. Immediately prior to

polymerization, 0.6µL of tetramethylethylenediamine (TEMED) was added to the PAm solution. 4µL of this complete PAm solution was applied to a new 22x22mm square glass coverslip and sandwiched with the treated 12mm round coverslip, while another 4 µL was applied to a treated 24x50 rectangular coverslip and sandwiched with a new, untreated 12mm round coverslip. These were placed in a humidity chamber and allowed to polymerize for 20 minutes. Next, a razor blade was used to clip the two coverslips apart. The PAm-coated glass was kept hydrated in water to preserve the PAm until further use.

3.3) PDMS solution preparation for fluidics chamber

Poly(dimethylsiloxane) (PDMS; Sylgaard 184; Dow Corning, Midland, MI, USA) was obtained and prepared by mixing a 10:1 ratio by mass of base to curing agent. This solution was thoroughly mixed for 3 minutes prior to it being poured gently on top of the silicone wafer containing PAm-coated 12mm glass coverslips in a 15cm petri dish. Once the PDMS was level and an even distribution was achieved, it was degassed in a vacuum chamber for approximately 30 minutes to remove all bubbles. The PDMS was then incubated overnight at 37ºC for curing.

3.4) Synthesis of LAP

First, 2,4,6-trimethylbenzoyl chloride was mixed drop-by-drop with an equal molar solution of dimethyl phenylphosphonite under argon while stirring at room temperature. Next, the temperature of the reaction mixture was set to 50ºC after 18 hours. Then, lithium bromide mixed with 2-butanone was added to the reaction mixture in

excess, causing precipitation within 10 minutes. After precipitation, the temperature was again cooled to room temperature and left for 4 hours. Next, to ensure complete removal of excess lithium bromide, the precipitate was collected by filtration and washed three times using 2-butanone. Finally, the product was dried using a vacuum to remove excess 2-butanone, yielding lithium phenyl-2,4,6-trimethylbenoylphosphinate (LAP).

3.5) Synthesis and purification of GelMA

Gelatin methacrylate (GelMA) was synthesized using a previously described protocol.[112] Briefly, 10 g of bovine skin gelatin (Sigma Aldrich, St. Louis, MO, USA) was mixed at 10%(w/v) with 100 ml phosphate buffered saline (PBS; Gibco, Billings, MT, USA) and stirred at 60˚C until fully dissolved. Next, methacrylic anhydride (MA; Sigma Aldrich) was added to the solution at a rate of 0.5 ml/min for a total of 8 ml. The solution was then stirred for 60 minutes at 50˚C. After being diluted 2x with warm PBS, the solution was dialyzed against distilled water using 12-14 kDa cutoff dialysis tubing (Spectrum Laboratories, Rancho Dominguez, CA, USA) for one week (3 times/day water change) at 40˚C to remove the unreacted methacrylic anhydride and methacrylic acid from the solution. Next, the GelMA solution was frozen using liquid nitrogen and lyophilized in a freeze dryer for 4 days before being stored at -80˚C until usage. The dried GelMA was further purified using column chromatography with a Sephadex G-25 column (GE Healthcare Life Sciences, Pittsburgh, PA, USA) and lyophilized.

3.6) 3D cardiac microtissues within microfluidic device

To create the 3D cardiac microtissues on a chip, we integrate 3D photopatterning technology with microfluidics. The device can be roughly described as containing an inner circular chamber composed of tri-layer hydrogels with microchannels leading to and from the chamber. To this end, a photomask with the desired designs were generated and this photomask was used to fabricate corresponding silicone wafers. The overall device fabrication is given in Fig. 1.

Poly-acrylamide (PAm) hydrogels embedded with 200 nm diameter green fluorescent particles were polymerized on glutradehyde-treated coverslips. Two such hydrogel-laden coverslips were generated –12 mm diameter round coverslips and 24 x 50 mm rectangular coverslips (Fig. 4A). The gluteraldehyde treatment was used to ensure strong bonding between the coverslip and the hydrogel. Next, 4.0 μL of DI H_2O was pipetted onto the circular chamber engraved on the etched silicon wafer, prior to placing the PAm hydrogel-tethered round coverslip on top of the water droplet (Fig. 4B). A 10:1 ratio of base to curing agent of polydimethylsiloxane (PDMS; Sylgard 184), was degassed and then gently poured over the wafer and coverslip, and incubated overnight at 37ºC for curing. The PDMS was then detached from the wafer and now contained the embedded hydrogel-tethered coverslip, with the hydrogel side exposed. We then punctured holes in the PDMS to provide inlet and outlet flow paths. Following that, we exposed both the PDMS and the rectangular coverslip described in step 1A to UV-Ozone treatment (Fig. 4C). The hydrogels attached on the PDMS mold and the rectangular coverslips were protected from deep UV by covering the hydrogels with 12 mm coverslips marked with dark ink. The circular depression within the PDMS is aligned

with the hydrogel tethered onto the rectangular coverslip and pressed into contact. This is incubated at 37ºC overnight to allow the PDMS to chemically and irreversibly bond to the glass, thereby forming the device as depicted in Figure 4D. The inlet and outlet openings of the fluidics device were sealed with tape to prevent the dehydration of the hydrogels within the device. Following bonding, phosphate-buffered saline (PBS) is flushed into the chamber on the subsequent day to equilibrate the hydrogel to physiological pH and osmolarity.

Isolated primary neonatal cardiomyocytes were mixed with 8.5% wt/v GelMA solution containing 0.01% wt/v Ascorbic acid and 2 mM LAP. This solution was injected into the fluidics chamber (Fig. 4D) and the photomask containing the ellipse or hexagon patterns was placed under the circular chamber of the device. The GelMA solution was photopolymerized using a UV light source with an excitation wavelength of 365 ± 40 nm (Fig. 4G). The regions of the hydrogel precursor solution exposed to UV light polymerized rapidly, thereby forming the microtissues with cells encapsulated within (Fig. 4E). The unreacted hydrogel precursor solution was removed from the fluidics chamber by injecting PBS in excess (Fig. 4F). Thus, the 3D heart-on-chip device with patterned microtissues between hydrogels was created (Fig. 4G). The device was then perfused with cardiomyocyte growth media and incubated at 37ºC and 10% CO_2 culture conditions. The cell encapsulation procedure is cytocompatible.

3.7) Laser scanning Confocal microscopy for 3D imaging

The sample used for the 3D Confocal imaging of the acellular GelMA patterned structures within the microfluidics device was made with green fluorescent beads

embedded within the polyacrylamide gels, and with red fluorescent beads in the GelMA hydrogel. An Olympus UMPlanFl 10x water immersion objective lens mounted onto a Leica SP5 microscope was used for imaging. The scan speed was set to 400Hz, with z-step size of 0.74um. The green beads were visualized using the 488nm laser, the 594nm laser was used to visualize the red beads. Sequential scanning was utilized to individually image the green and red fluorescent beads to minimize unwanted excitation of the channels.

3.8) Immunofluorescent staining within fluidics device

The microfluidic chip was removed from the 37ºC incubator and disconnected from the media input before being flushed through with PBS twice to clean out remaining media within the circular chamber. Next, formaldehyde solution (1:10 dilution in PBS) was flushed into the device and incubated for 10 minutes at room temperature. After flushing three times with PBS at 10-minute intervals, collagen type II solution (0.1% in PBS) was flushed into the device and incubated for 15 minutes at room temperature. After flushing three times with PBS at 10-minute intervals, the device was flushed with blocking buffer (3% bovine serum albumin + 0.1% Triton-X 100) and incubated for 45 minutes at room temperature. Anti-Connexin-43 rabbit antibody (Sigma Aldrich, St. Louis, MO, USA) diluted 1:400 in blocking buffer was then flushed into the device and the device was incubated in a humidity chamber for 2 hours. After flushing three times with PBS at 10-minute intervals, Alexa Fluor 488 goat anti-rabbit antibody (1:250 dilution in blocking buffer; Life Technologies, Carlsbad, CA, USA) was flushed into the device and incubated for 2 hours. After flushing three times with PBS at 10-minute

intervals, CellMask (Life Technologies, Carlsbad, CA, USA) was flushed into the device and the inlet and outlet ports were sealed with tape prior to imaging.

3.9) Time-lapse imaging of cardiomyocyte-embedded structures during contraction

The contraction of the GelMA structures embedded with cardiomyocytes was imaged using 40x UMPlanFl lenses mounted onto a spinning disk Confocal microscope. The fluorescent particles at the top surface of the PAm hydrogel below the GelMA structures were acquired at ~ 20 frames per second for 90 seconds duration. Three fields of view were acquired to encompass the entire GelMA structure. The time-lapse images from these fields of view were temporally synchronized to account for latency in the deformations between each field. These images were then stitched using custom Matlab software to obtain the entire image containing the GelMA structures.

3.10) Calculation of contractile stresses

To quantify the contractile stresses generated by the cardiomyocytes, we exploited the propagation of stresses originating from the GelMA structures to the PAm hydrogels. Since GelMA is derived from collagen and is susceptible to degradation, the stresses cannot be accurately determined from visualization of the GelMA structures themselves due to their changing material properties. However, the inert properties of PAm hydrogels allow for the calculation of stresses under the assumption of linearly isotropic material properties.[113] In addition, we used a measured value of 8.5 kPa for the elastic modulus of the PAm hydrogel and 0.45 for Poisson's ratio as indicated in literature.[114]

By treating the PAm hydrogel as a 3 dimensional block tethered at the bottom in mechanical equilibrium, we used a finite element (FE) approach to solve a series of elastostatics equations. On the sides of the 3D block, we assumed the material to be stress-free while we imposed displacement boundary conditions in the x- and y-directions on the top surface of the PAm hydrogel. We neglected the normal deformations since our results indicated negligible normal displacements. To obtain the input for the boundary condition at the top surface of the gel, we quantified the displacement of the hydrogel by tracking the fluorescent particles embedded within the network using particle image velocimetry (PIV).[115] The FE mesh was constructed to have 100 elements in the x- and y-direction and 60 elements in the z-direction. The contraction of the microtissues was reported as peak traction stress.

Using this approach, we obtained fluorescent images of the green beads embedded within PAm at a frequency of 9 frames per second to capture the contraction profile of the cardiomyocytes at 20x magnification. With the goal of obtaining the reference state, the embedded cells were removed from the GelMA structure afterwards using a dissolving solution comprised of ammonium hydroxide and Triton-X 100. After the removal of cells, the PAm gels embedded with beads were reimaged to obtain the reference state. We obtained the displacement field using PIV by comparing the reference state to the images captured during the contraction of the cells. Using our FE approach, we calculated the traction stress field caused by the cellular forces.

Chapters 1, 3, 4 and 5, in part, are currently being prepared for submission for publication of the material. Bhullar, Ivneet S; Aung, Aereas; Theprungsirikul, Jomkuan; Davey, Shruti K; Lim, Han L; Chiu, Yu-Jui; Lo, Yu-Hwa; McCulloch, Andrew; Varghese, Shyni. The dissertation/thesis author was the primary investigator and author of this material.

Chapter 4: RESULTS

4.1) Fabrication and characterization of the device

To create a perfused cardiac tissue model with real-time force readouts, we have created a microfluidic device with a vertical arrangement of tri-layer hydrogel structures. Figure 4 summarizes the fabrication of the device including cell encapsulation. An integral part of the device is the 3D patterned cell-laden hydrogels sandwiched between two linearly elastic non-degradable hydrogels. In this proof-of-concept study, we used GelMA for cell encapsulation and polyacrylamide hydrogels as the top and bottom layers to act as sensors for contractile stress. Prior to cell encapsulation an acellular method involving fluorescent beads with different excitation levels was used to optimize and characterize the tri-layer device (Fig. 5). The 3D patterned GelMA structures sandwiched between the PAm layers can be designed to take any shape, which can be controlled by the photomask design. We have tested out ellipsoid and hexagonal structures. We incorporated 200 nm red fluorescent particles in GelMA solution prior to polymerization to visualize the structures within the device. For the polyacrylamide layer, gels were polymerized in presence of 200 nm green fluorescent particles. The formed structure was imaged using a spinning disk Confocal microscope and the images were reconstructed to obtain a 3D representation of the device (Fig. 5). The X-Z image section illustrates the GelMA structures with red particles of approximately 120 μm thickness encased above and below by the PAm hydrogels of 70 μm thickness filled with green particles (Fig. 5A). The X-Y sections at the indicated Z positions demonstrate the planar structure of the PAm hydrogel along with the structure of the GelMA gels (Fig. 5B, C). The 3D rendering

of these constructs (Fig. 5D, E) shows the structures of GelMA and the tri-layer composite.

4.2) Encapsulation of cardiomyocytes within the device

The neonatal mouse cardiomyocytes were encapsulated within the GelMA structures by photopolymerization, where the cardiomyocyte-laden GelMA structures are housed within the internal circular chamber (Fig. 4D-G). For a 12mm diameter inner chamber, we were able to create an array of around 200 cardiac micro-tissues of dimensions 400μm x 133μm x 120 μm. The cell-laden GelMA structures were sandwiched between two thin layers of polyacrylamide (PAm) hydrogels (~70 μm thickness) containing 200 nm fluorescent nanoparticles. The device was infused with cardiomyocyte maintenance media and the cell function was monitored as a function of time. The encapsulated cells were found to contract starting day 2 and maintained a coordinated contraction for up to 14 days (maximum allowed experimental length time). DIC images of the GelMA structures at various culture time points is shown in Figure 6A. Since the isolation of cardiomyocytes also contains a small population of fibroblasts, we labeled the cells using CellMask, which stains all cells. To identify the encapsulated cardiomyocytes, we used Connexin-43, a cardiac-specific marker. Confocal sections of the stained cells indicated that the cells positive for Connexin-43 were located within the interior of the structures with the fibroblasts (identified by a negative stain for Connexin-43) confined mostly on the periphery (Fig. 6B).

4.3) Real-time contractile force measurements

Cardiomyocytes entrapped within the GelMA structures were cultured for 7 days within the microfluidics device prior to assessing their contractile forces. We first obtained the deformation of the PAm gels, measured by the displacement of the embedded particles, in response to the contractile forces generated by the encapsulated cells. The position of the embedded fluorescent particles after the removal of the cells was used as a reference state. We quantified the contractile stresses using this displacement field and finite element analysis. The left panel in Figure 7A illustrates the displacement field of the particles and the corresponding traction stresses at various time points (T1-T4) during a contraction cycle of the cardiomyocytes. The traction forces were found to exhibit stresses that are higher along the major axis of the ellipse compared to the stresses along the minor axis. The peak traction stress, calculated by averaging the traction stress values immediately surrounding the region of highest stress along the major axis of the ellipse, for oscillatory contraction cycles is depicted in Figure 7B as a function of time. Furthermore, our traction force analysis shows positive stress values even in the relaxed state of the contractile cycle, which is termed as residual stress. The residual stress was determined by comparing the stress exerted by the cells during the relaxation phase of the contractile cycle to the absolute reference state obtained by removing the cells from the system.

4.4) Proof-of-concept with epinephrine

To prove the ability of this system to exhibit cardiac-specific effects when exposed to small molecules or drugs, we perturbed the contraction cycles by

supplementing the culture with 0.1 μg/ml of epinephrine, which is known to increase the frequency and amplitude of cardiac tissue contractions.[116] The contractile stress profile of cardiac cell-laden structures exposed to epinephrine was calculated to determine the effect of epinephrine on the cardiac cells. Figure 7B shows the increased frequency and amplitude of contraction cycles when the cells are exposed to epinephrine. While the presence of epinephrine increased the force amplitude, it slightly decreased the residual stress observed at the relaxation phase of the contraction cycle when compared to control (Fig. 7C).

Chapters 1, 3, 4 and 5, in part, are currently being prepared for submission for publication of the material. Bhullar, Ivneet S; Aung, Aereas; Theprungsirikul, Jomkuan; Davey, Shruti K; Lim, Han L; Chiu, Yu-Jui; Lo, Yu-Hwa; McCulloch, Andrew; Varghese, Shyni. The dissertation/thesis author was the primary investigator and author of this material.

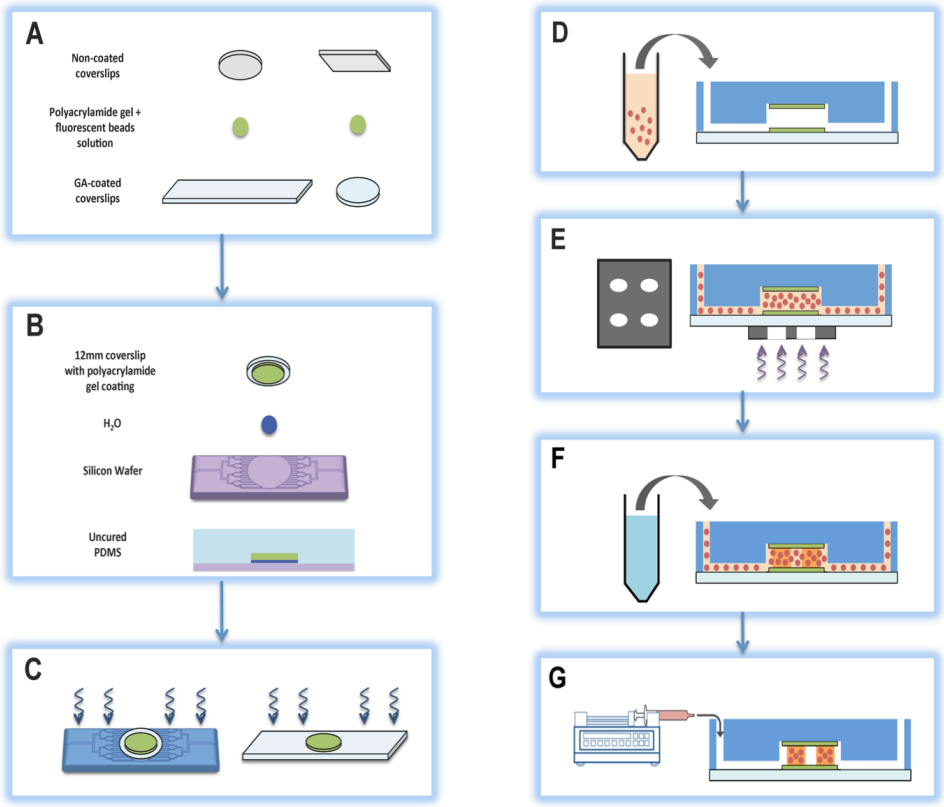

Figure 4: Fabrication of microfluidic device and three-dimensional encapsulation of cardiomyocytes. (A) Two PAm hydrogels were polymerized by sandwiching the precursor solution mixed with fluorescent nanoparticles between regular and GA-treated coverslips. (B) A small droplet of DI water was deposited onto a silicon wafer prior to placing a PAm hydrogel tethered on a circular coverslip on top. Polydimethylsiloxane (PDMS) solution containing the curing agent (10:1 ratio) was gently poured onto the construct and cured at 37ºC overnight. (C) The PDMS mold attached to the PAm hydrogel was removed from the wafer and inlet and outlet ports for the device were generated. This construct was bonded to a rectangular coverslip tethered to a PAm hydrogel using UV/Ozone treatment. Care was taken to align the two hydrogels during the process. The device was placed in 60ºC for an hour within a humidity chamber prior to moving to a 37ºC chamber overnight. (D) Cells mixed with GelMA, and a photoinitiator were injected into the chamber. (E) A patterned transparency photomask was placed underneath the bottom glass coverslip before exposing the region to UV light for polymerization. (F) PBS solution was injected into the device to remove GelMA mixture in the non-polymerized region. (G) The device was attached to a syringe pump containing maintenance media and placed in a 37ºC incubator to culture the cells encapsulated within patterned GelMA matrices.

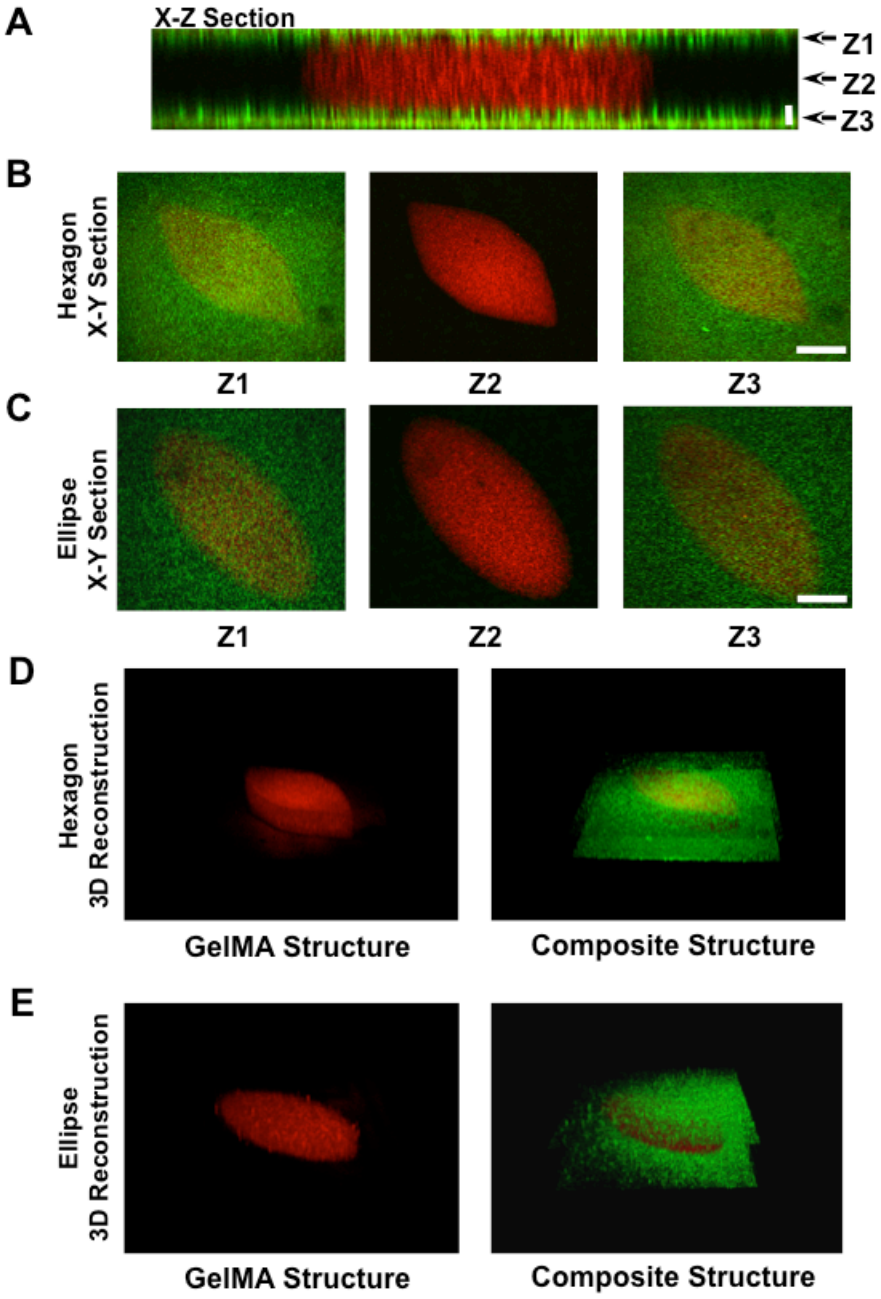

Figure 5: Characterization of patterned ellipsoid and hexagonal hydrogel structures within microfluidic device. Z-stack images of the hydrogels were obtained using a laser scanning Confocal microscope. The X-Z cross-section (A) and the corresponding X-Y planes at different Z locations (B and C) are shown for hexagonal and ellipsoid geometries. GelMA and the PAm hydrogels were embedded with red and green fluorescent particles, respectively, to visualize these structures. Vertical scale bar: 10 μm. Horizontal scale bars: 100 μm. (D and E) 3D rendering of the GelMA hydrogel (Left Panels) and the composite structure showing both the PAm and GelMA hydrogels (Right Panels) are shown for hexagonal and ellipsoid geometries.

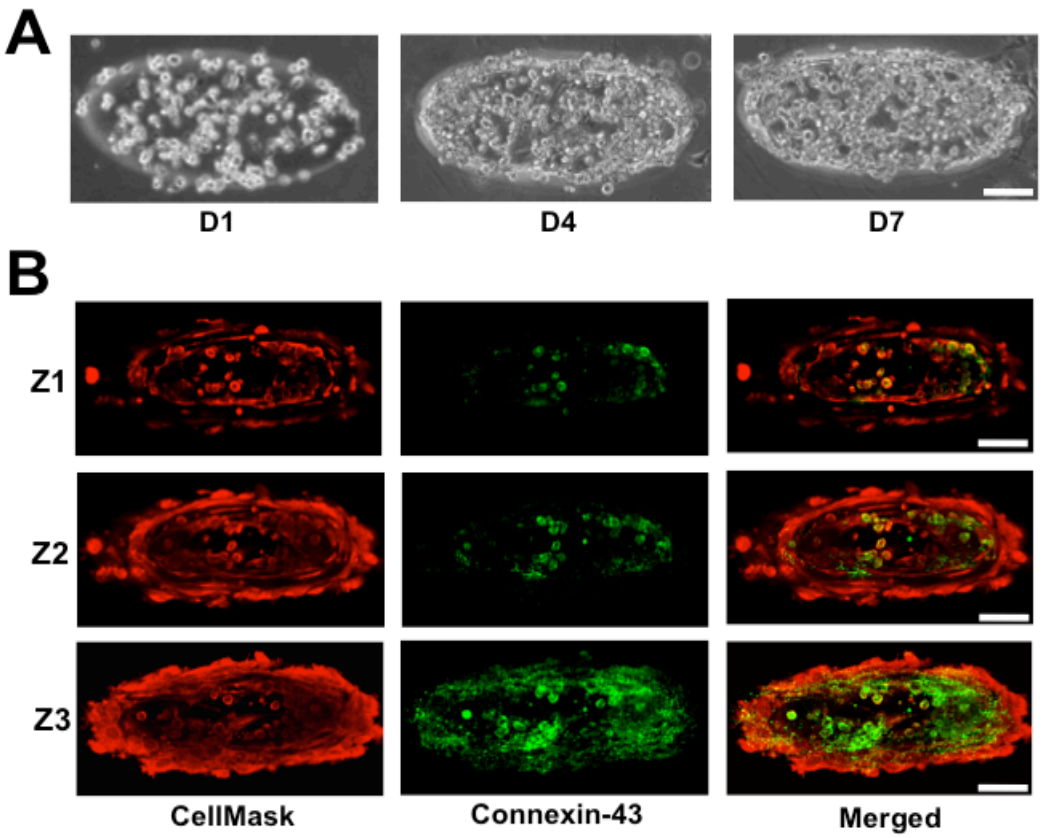

Figure 6: Organization of encapsulated cells within GelMA structures. (A) Cell density within the GelMA structures increased as a function of culture time. (B) X-Y Confocal sections of cells ubiquitously stained with CellMask and immunostained for Connexin-43. Connexin-43 negative staining amongst the encapsulated cells suggests the presence of cardiac fibroblasts. The Confocal sections proceed from the top, Z1, to the bottom, Z3, of the GelMA structures. Scale bars: 100 μm.

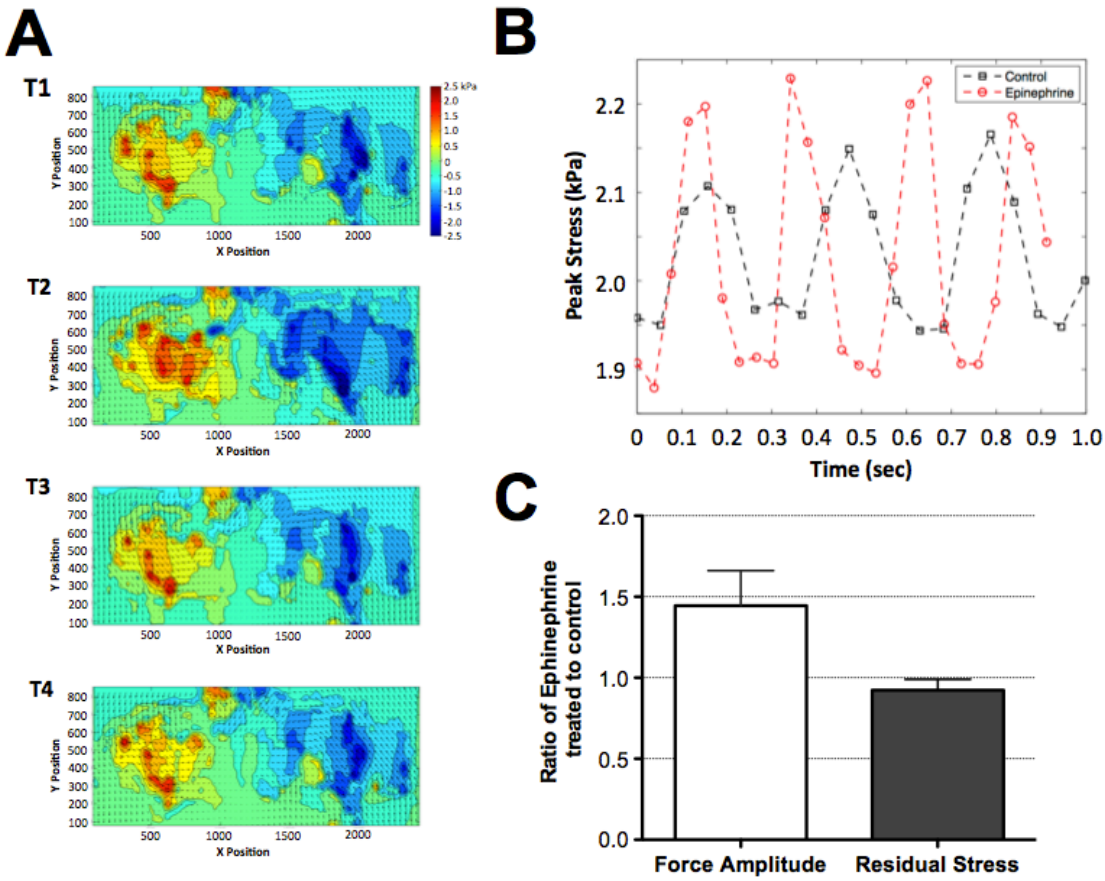

Figure 7: Quantification of contractile stresses within GelMA structures. (A) The planar displacements, shown as a vector field, and the traction stresses along the major axis of the GelMA structures, shown as a heat map, were measured from the PAm hydrogels. The times associated with each graph, T1 through T4, are shown in (B). The X- and Y- axis of the graphs indicate the physical location of the measured quantities while the values within the heat map are indicated by the color bar. (B) A representative plot of the peak traction stress as a function of time in absence (black squares) and presence (red circles) of epinephrine. The stresses along the major axis of the GelMA structures were used for determining the peak value. (C) The ratio of force amplitude and residual stress in the presence of epinephrine to absence of epinephrine measured from multiple microtissues. Values lower than or higher than 1 indicate a decrease or increase in force amplitude and residual stress, respectively, while a value of 1 suggests the lack of change.

Chapter 5: DISCUSSION

Organ-on-chip platforms have become increasingly popular to study tissue-environment interactions *in vitro* and to investigate the effects of small molecule and environmental perturbations. These platforms have been able to address many of the shortcomings of static 2D cell culture and animal model testing for determining drug toxicity and efficacy. However, precisely controlling cell seeding in 3D cell-laden constructs within a perfusion-based device that allows for real-time contractile force readout has not yet been achieved. Here, we have built a device that consists of arrays of viable 3D cardiac cell structures with the ability to measure cardiac cell-generated contractile forces. Additionally, we have shown the ability of these 3D cardiac cell cultures to respond appropriately to small molecules with known cardiac effects, using epinephrine as a proof-of-concept.

The immunofluoresecent staining and measurement of contractile forces indicate healthy cardiac microtissues that can be studied for cardiac-specific tissue-environment interactions. Connexin-43, found abundantly in cardiac tissue, is a member of a family of proteins that assemble to form gap junctions across the plasma membrane of cells, allowing for the exchange of small molecules, ions and secondary messengers.[117] Staining for connexin-43, we see that the cardiac cells form gap junctions that allow for the coordinated contraction within each construct. However, during the primary cell isolation process, it is difficult to isolate pure cardiomyocytes, leading to a heterogeneous cell mixture that includes primary fibroblasts in addition to cardiomyocytes. It has been shown that gap junctions formed by connexin-43 also facilitate the coupling of fibroblasts and cardiomyocytes. This allows for the propagation of electrical signals through the

fibroblasts, leading to the coordinated contraction of cardiomyocytes separated by fibroblasts, even though the fibroblasts themselves do not generate cardiac action potentials.[118] Recently it has also been shown that fibroblasts may have critical cardiac electrophysiological functions beyond acting as passive barriers that allow for normal electrical signal propagation.[45] Thus, the presence of fibroblasts in these 3D cell-laden structures is essential to normal tissue formation and function. The staining images for connexin-43 as well as visual observation of coordinated contractions indicate functional cardiac structures.

We have also quantified the contraction profile of the cardiomyocytes by analyzing the forces transmitted from the GelMA structures onto the PAm hydrogel. We calculated the transduced traction stresses within the inert PAm hydrogel to circumvent the inaccuracies in measurements associated with cell-induced ECM remodeling of collagen-derived GelMA structures. Since PAm maintains consistent material properties throughout the experiment in contrast to the GelMA constructs, it is an ideal candidate for such a far-field approach. However, this far-field concept can have several drawbacks, including the decay of force transduced with increasing distance from each contracting cell. This was circumvented by seeding each construct with cardiomyocytes at a very high density, ensuring the presence of cells throughout the construct, and measuring the force generated by the entire 3D construct. This allowed for a force readout that was consistent with the force generated by the entire structure rather than one that was dominated by any particular cell. Additionally, forces were measured by examining the displacement of nanoparticles very close to the periphery of the GelMA construct, minimizing the decay of force readout. Further, the contractile force generated

by each construct was compared only to itself before and after the introduction of epinephrine, ensuring an accurate measurement of the effect of the small molecule on the structure.

Within our system, the GelMA structures are placed between two PAm hydrogels tethered onto the top and bottom surfaces of the flow chamber. For our force calculations, we have only analyzed the deformations observed within the bottom PAm hydrogel layer due to technical limitations. With an inverted microscope, the presence of the GelMA structures causes light diffraction thus the embedded fluorescent particles above the GelMA hydrogels cannot be imaged. On the other hand, an upright microscope can image the fluorescent particles without experiencing light diffraction. However, the thickness of the PDMS chamber exceeds the working distance of the microscope lenses that are used to image the particles from the top of the device. Nevertheless, we have chosen to use PAm hydrogels with the same rigidity (~ 8.5 kPa) and thickness (~ 150μm) at both the top and bottom surface to eliminate the possibility of mechanical edge effects on the cardiomyocytes caused by tethering the GelMA structures to a rigid glass surface.[119]

The response of the cell-laden structures to pharmaceutical intervention further characterizes the constructs as having cardiac-specific responses. The effect of epinephrine was studied by analyzing the difference in contraction frequency and contractile force generated by a construct in the presence and absence of the small molecule. The increased magnitude and frequency of contraction with the addition of epinephrine (0.1 μg/ml) proved the utility of this system for studying the cardiac-specific effect of a small molecule. Further, the ability to visualize these effects and take

contractile force measurements in real-time provides for a system that can determine both immediate and long-term drug effects up to 14 days without perturbation of the system. These capabilities make this model especially attractive for drug screening as it addresses shortcomings of current models. Specifically, real-time analysis cannot be performed in animal model testing while many current organ-on-chip systems lack real-time force readout as well.[54,55,120]

Further, we have calculated the absolute values of the traction stresses exerted by the 3D cell-laden structures by utilizing a mechanical reference state in which the cardiomyocytes have been completely removed from the system. With this approach, we investigated the changes in the residual stresses that the cardiomyocytes apply in the presence of drugs. When the cells were exposed to epinephrine, the residual stress was seen to decrease, indicating a lower relaxed state with increased contractility. This lower relaxed state could be the result of stretching of the GelMA material caused by the increased magnitude of contractile force. Monitoring such changes in residual stresses may lead to novel insights into the effects of drugs on cell-ECM interactions since this system allows for the quantification of force exerted by cardiomyocytes on the surrounding ECM at the cellular level.

The system built and characterized here holds potential for many translational applications in healthcare. Due to the unique control this device affords for cellular spatial arrangement along with its adaptability to work with multiple cell types, the encapsulation of human umbilical vein endothelial cells (HUVECs) in a geometry resembling the human circulatory system between the cardiac microtissues would create a flow system with 3D vascularized cardiac structures, recapitulating the *in vivo*

environment even more closely. Moreover, the incorporation of cardiomyocytes derived from human-induced pluripotent stem cells (hiPSCs) would increase the value of this system as a human-specific *in vitro* 3D cardiac model. Further, fabricating this device with hiPSCs opens the door for personalized drug testing to assess patient-specific responses to certain pharmaceuticals since hiPSCs can be generated using a patient's own adult cells.[35] Additionally, by inducing cardiomyopathies and other cardiac conditions within this device, existing heart-on-chip disease models[22,26,27] can be improved by recapitulating disease states in this 3D flow system.

Thus, we have produced a 3D heart-on-chip system in which we have successfully created and characterized functional cardiac structures. We have proven the drug-specific response of these constructs to epinephrine, showing the promise of this device for small molecule drug testing. These results must next be replicated using hiPSCs to study human-specific drug effects. Additionally, this system offers the potential for improvement on existing heart-on-chip disease models by providing a platform to create more physiologically relevant 3D disease models. Combining its features, this device provides an easy-to-use, cost-effective system that has the potential to dramatically improve *in vitro* 3D culture models.

Chapters 1, 3, 4 and 5, in part, are currently being prepared for submission for publication of the material. Bhullar, Ivneet S; Aung, Aereas; Theprungsirikul, Jomkuan; Davey, Shruti K; Lim, Han L; Chiu, Yu-Jui; Lo, Yu-Hwa; McCulloch, Andrew; Varghese, Shyni. The dissertation/thesis author was the primary investigator and author of this material.

Chapter 6: CONCLUSION AND FUTURE DIRECTIONS

Here, we have detailed the design, fabrication and utility of 3D cardiac cell-laden structures housed within a microfluidic device as an *in vitro* cardiac model. The ability of the tri-layer hydrogel system within the device to provide real-time contractile force readout *in situ* makes it especially attractive. Further, the 3D patterning technology used to encapsulate cells within the device allows for spatial control of the generation of cell-laden structures while also potentiating the incorporation of multiple cell types. Also, the encapsulation of the cardiomyocytes within a GelMA hydrogel matrix provides a 3D microenvironment that allows for cell adherence, migration, proliferation and organization. Thus, our system provides the following benefits:

1. Three-dimensional (3D) microenvironment that closely mimics native cell-cell and cell-ECM interactions
2. Microfluidic channels that provide convective transport of nutrients and waste, recapitulating the role of native microvasculature
3. 3D patterning technology that allows for precise spatial distribution of multiple cell types within the device
4. Unique tri-layer hydrogel design that allows for the calculation of contractile stresses generated by the cardiac cells *in situ* with the use of a far-field approach and finite element analysis

Furthermore, these qualities of the device were demonstrated through:

- The 3D characterization of the device, showing the vertical tri-layer hydrogel system in which a cell-laden GelMA structure is sandwiched between two inert PAm structures, which include embedded fluorescent nanoparticles

- The immunostaining for Connexin-43, a gap junction protein and specific marker for cardiomyocytes, that shows the presence of cardiomyocytes throughout the construct as well as the presence of cardiac fibroblasts
- The quantification of the contractile forces generated by the 3D cardiac cell-laden structures in the absence and presence of epinephrine, a known agonist that causes increased contraction frequency and force magnitude

The development of *in vitro* cardiac drug screening platforms has progressed at a rapid pace in the past decade. Moving on from previous 2D monolayer cell culture models, researchers have created many freestanding 3D *in vitro* cardiac models that have demonstrated characteristics of cardiac tissue environments. Thavandiran et. al. is one such group that was able to create more physiologically relevant 3D tissues with precise design criteria to mimic the native environment. However, the innate reliance on static culture associated with 3D *in vitro* tissue models within an open-well configuration makes them unattractive candidates compared to dynamic, flow-based culture models. Whereas such static culture models provide a fluctuating supply of nutrients and potential drug candidates as the media supply is changed periodically, flow-based culture models provide a continuous supply of nutrients and pharmacological agents of interest, thus better recapitulating the circulatory system. Based on this principle, researchers began exploring the intersection between microfluidics and biology, leading to the development of organ-on-chip systems. Heart-on-chip systems, being a relatively new technology, have a long road of progress ahead. Agarwal et. al. and Mathur et. al. have been able to make significant progress in this field, with each improving on previous designs and each

having its respective downfalls as well. The use of muscular thin film technology (MTF) by Agarwal et. al. allows for the quantification of forces generated by 2D monolayers within a microfluidic system; however, such a 2D environment is not in tune with the native environment of cardiac cells. The unique design by Mathur et. al. recreates a 3D microenvironment within a microfluidic device; however, it does not have the capability of allowing the functional measurement of contractile forces, an important indicator of cardiac cell function.

Thus, our design and development of a microfluidic cardiac device described in this thesis serves as a proof-of-concept of a system that combines 3D tissue environments with dynamic cell culture and the ability to calculate contractile forces, something that is critical to assay cardiac functionality. Such a design is novel and progresses the field of heart-on-chip systems for drug screening even further by providing an easy-to-use, cost-effective device with the capability of providing multiple modes of analysis. As the cost of drug development continues to increase due to late stage failures in clinical trials, the inadequacies of preclinical drug screening is further highlighted. With the standard of 2D monolayer cell cultures and *in vivo* animal models no longer considered sufficient to identify viable drug candidates while weeding out unattractive ones, heart-on-chip systems promise to provide more physiologically relevant alternatives.

The findings of this thesis lead to many emerging studies of interest. Pursuing these studies would provide valuable insight into the potential of our device as a cardiac drug-screening platform. These future studies include:

1. Study the effect of incorporating HUVECs for creating microvasculature between the 3D cardiac tissues, thus better mimicking native environments.

2. Study the effects of creating 3D GelMA cell-laden constructs of different geometries on cell-induced remodeling, cell proliferation and cardiac functionality. One aspect of interest here could be investigating how the major axis of contraction changes with changing geometries.
3. Investigate the role of cardiac fibroblasts in creating functional cardiac tissues by varying the ratio of cardiomyocytes to cardiac fibroblasts seeded within the constructs in the device.
4. Incorporate human induced pluripotent stem cells (hiPSCs) as a cell source to create a human-specific *in vitro* cardiac model.
5. Study the human-specific effect of various drugs on this device using hiPSCs as a cell source. Use this information to evaluate this device as a tool for supplementing and eventually replacing animal studies.
6. Create cardiac disease models (using hiPSCs of a diseased background) in this system to provide a platform for the study of the pathophysiology of various disease states.
7. Integrate this model with other organ systems to create a "human-on-chip" to study systemic effects of various pharmacological agents.

REFERENCES

1 Heylman, C., Sobrino, A., Shirure, V. S., Hughes, C. C. & George, S. C. A strategy for integrating essential three-dimensional microphysiological systems of human organs for realistic anticancer drug screening. *Experimental biology and medicine* **239**, 1240-1254, doi:10.1177/1535370214525295 (2014).

2 Haycock, J. W. 3D cell culture: a review of current approaches and techniques. *Methods in molecular biology* **695**, 1-15, doi:10.1007/978-1-60761-984-0_1 (2011).

3 Kim, J., Park, J., Na, K., Yang, S., Baek, J., Yoon, E., Choi, S., Lee, S., Chun, K., Park, J. & Park, S. Quantitative evaluation of cardiomyocyte contractility in a 3D microenvironment. *Journal of biomechanics* **41**, 2396-2401, doi:10.1016/j.jbiomech.2008.05.036 (2008).

4 Wang, F., Weaver, V. M., Petersen, O. W., Larabell, C. A., Dedhar, S., Briand, P., Lupu, R. & Bissell, M. J. Reciprocal interactions between beta1-integrin and epidermal growth factor receptor in three-dimensional basement membrane breast cultures: a different perspective in epithelial biology. *Proceedings of the National Academy of Sciences of the United States of America* **95**, 14821-14826 (1998).

5 Anders, M., Hansen, R., Ding, R. X., Rauen, K. A., Bissell, M. J. & Korn, W. M. Disruption of 3D tissue integrity facilitates adenovirus infection by deregulating the coxsackievirus and adenovirus receptor. *Proceedings of the National Academy of Sciences of the United States of America* **100**, 1943-1948, doi:10.1073/pnas.0337599100 (2003).

6 Beningo, K. A., Dembo, M. & Wang, Y. L. Responses of fibroblasts to anchorage of dorsal extracellular matrix receptors. *Proceedings of the National Academy of Sciences of the United States of America* **101**, 18024-18029, doi:10.1073/pnas.0405747102 (2004).

7 Cukierman, E., Pankov, R., Stevens, D. R. & Yamada, K. M. Taking cell-matrix adhesions to the third dimension. *Science* **294**, 1708-1712, doi:10.1126/science.1064829 (2001).

8 Meshel, A. S., Wei, Q., Adelstein, R. S. & Sheetz, M. P. Basic mechanism of three-dimensional collagen fibre transport by fibroblasts. *Nature cell biology* **7**, 157-164,doi:10.1038/ncb1216(2005).

9 Walpita, D. & Hay, E. Studying actin-dependent processes in tissue culture. *Nature reviews. Molecular cell biology* **3**, 137-141, doi:10.1038/nrm727 (2002).

10 Philip, M., Benatar, M., Fisher, M. & Savitz, S. I. Methodological quality of animal studies of neuroprotective agents currently in phase II/III acute ischemic stroke trials. *Stroke; a journal of cerebral circulation* **40**, 577-581, doi:10.1161/STROKEAHA.108.524330 (2009).

11 Bottini, A. A. & Hartung, T. Food for thought... on the economics of animal testing. *Altex* **26**, 3-16 (2009).

12 Boudou, T., Legant, W. R., Mu, A., Borochin, M. A., Thavandiran, N., Radisic, M., Zandstra, P. W., Epstein, J. A., Margulies, K. B. & Chen, C. S. A microfabricated platform to measure and manipulate the mechanics of engineered cardiac microtissues. *Tissue engineering. Part A* **18**, 910-919, doi:10.1089/ten.TEA.2011.0341 (2012).

13 Baar, K., Birla, R., Boluyt, M. O., Borschel, G. H., Arruda, E. M. & Dennis, R. G. Self-organization of rat cardiac cells into contractile 3-D cardiac tissue. *FASEB journal : official publication of the Federation of American Societies for Experimental Biology* **19**, 275-277, doi:10.1096/fj.04-2034fje (2005).

14 Linder, P., Trzewik, J., Ruffer, M., Artmann, G. M., Digel, I., Kurz, R., Rothermel, A., Robitzki, A. & Temiz Artmann, A. Contractile tension and beating rates of self-exciting monolayers and 3D-tissue constructs of neonatal rat cardiomyocytes. *Medical & biological engineering & computing* **48**, 59-65, doi:10.1007/s11517-009-0552-y (2010).

15 Khademhosseini, A., Eng, G., Yeh, J., Kucharczyk, P. A., Langer, R., Vunjak-Novakovic, G. & Radisic, M. Microfluidic patterning for fabrication of contractile cardiac organoids. *Biomedical microdevices* **9**, 149-157, doi:10.1007/s10544-006-9013-7 (2007).

16 Thavandiran, N., Dubois, N., Mikryukov, A., Masse, S., Beca, B., Simmons, C. A., Deshpande, V. S., McGarry, J. P., Chen, C. S., Nanthakumar, K., Keller, G. M., Radisic, M. & Zandstra, P. W. Design and formulation of functional pluripotent stem cell-derived cardiac microtissues. *Proceedings of the National Academy of Sciences of the United States of America* **110**, E4698-4707, doi:10.1073/pnas.1311120110 (2013).

17 Radisic, M., Park, H., Shing, H., Consi, T., Schoen, F. J., Langer, R., Freed, L. E. & Vunjak-Novakovic, G. Functional assembly of engineered myocardium by electrical stimulation of cardiac myocytes cultured on scaffolds. *Proceedings of the National Academy of Sciences of the United States of America* **101**, 18129-18134, doi:10.1073/pnas.0407817101 (2004).

18 Huh, D., Hamilton, G. A. & Ingber, D. E. From 3D cell culture to organs-on-chips. *Trends in cell biology* **21**, 745-754, doi:10.1016/j.tcb.2011.09.005 (2011).

19 Bhatia, S. N. & Ingber, D. E. Microfluidic organs-on-chips. *Nature biotechnology* **32**, 760-772, doi:10.1038/nbt.2989 (2014).

20 Mathur, A., Loskill, P., Shao, K., Huebsch, N., Hong, S., Marcus, S. G., Marks, N., Mandegar, M., Conklin, B. R., Lee, L. P. & Healy, K. E. Human iPSC-based Cardiac Microphysiological System For Drug Screening Applications. *Scientific reports* **5**, 8883, doi:10.1038/srep08883 (2015).

21 Agarwal, A., Goss, J. A., Cho, A., McCain, M. L. & Parker, K. K. Microfluidic heart on a chip for higher throughput pharmacological studies. *Lab on a chip* **13**, 3599-3608, doi:10.1039/c3lc50350j (2013).

22 Khanal, G., Chung, K., Solis-Wever, X., Johnson, B. & Pappas, D. Ischemia/reperfusion injury of primary porcine cardiomyocytes in a low-shear microfluidic culture and analysis device. *The Analyst* **136**, 3519-3526, doi:10.1039/c0an00845a (2011).

23 Grosberg, A., Alford, P. W., McCain, M. L. & Parker, K. K. Ensembles of engineered cardiac tissues for physiological and pharmacological study: heart on a chip. *Lab on a chip* **11**, 4165-4173, doi:10.1039/c1lc20557a (2011).

24 Cheng, W., Klauke, N., Sedgwick, H., Smith, G. L. & Cooper, J. M. Metabolic monitoring of the electrically stimulated single heart cell within a microfluidic platform. *Lab on a chip* **6**, 1424-1431, doi:10.1039/b608202e (2006).

25 Giridharan, G. A., Nguyen, M. D., Estrada, R., Parichehreh, V., Hamid, T., Ismahil, M. A., Prabhu, S. D. & Sethu, P. Microfluidic cardiac cell culture model (muCCCM). *Analytical chemistry* **82**, 7581-7587, doi:10.1021/ac1012893 (2010).

26 McCain, M. L., Sheehy, S. P., Grosberg, A., Goss, J. A. & Parker, K. K. Recapitulating maladaptive, multiscale remodeling of failing myocardium on a chip. *Proceedings of the National Academy of Sciences of the United States of America* **110**, 9770-9775, doi:10.1073/pnas.1304913110 (2013).

27 Wang, G., McCain, M. L., Yang, L., He, A., Pasqualini, F. S., Agarwal, A., Yuan, H., Jiang, D., Zhang, D., Zangi, L., Geva, J., Roberts, A. E., Ma, Q., Ding, J., Chen, J., Wang, D. Z., Li, K., Wang, J., Wanders, R. J., Kulik, W., Vaz, F. M., Laflamme, M. A., Murry, C. E., Chien, K. R., Kelley, R. I., Church, G. M., Parker, K. K. & Pu, W. T. Modeling the mitochondrial cardiomyopathy of Barth syndrome with induced pluripotent stem cell and heart-on-chip technologies. *Nature medicine* **20**, 616-623, doi:10.1038/nm.3545 (2014).

28 Rheinwald, J. G. & Green, H. Serial cultivation of strains of human epidermal keratinocytes: the formation of keratinizing colonies from single cells. *Cell* **6**, 331-343 (1975).

29 Green, H., Kehinde, O. & Thomas, J. Growth of cultured human epidermal cells into multiple epithelia suitable for grafting. *Proceedings of the National Academy of Sciences of the United States of America* **76**, 5665-5668 (1979).

30 O'Connor, N. E., Mulliken, J. B., Banks-Schlegel, S., Kehinde, O. & Green, H. Grafting of burns with cultured epithelium prepared from autologous epidermal cells. *Lancet* **1**, 75-78 (1981).

31 Bell, E., Ehrlich, H. P., Buttle, D. J. & Nakatsuji, T. Living tissue formed in vitro and accepted as skin-equivalent tissue of full thickness. *Science* **211**, 1052-1054 (1981).

32 Burke, J. F., Yannas, I. V., Quinby, W. C., Jr., Bondoc, C. C. & Jung, W. K. Successful use of a physiologically acceptable artificial skin in the treatment of extensive burn injury. *Annals of surgery* **194**, 413-428 (1981).

33 Yannas, I. V., Burke, J. F., Orgill, D. P. & Skrabut, E. M. Wound tissue can utilize a polymeric template to synthesize a functional extension of skin. *Science* **215**, 174-176 (1982).

34 Vacanti, J. P., Morse, M. A., Saltzman, W. M., Domb, A. J., Perez-Atayde, A. & Langer, R. Selective cell transplantation using bioabsorbable artificial polymers as matrices. *Journal of pediatric surgery* **23**, 3-9 (1988).

35 Takahashi, K. & Yamanaka, S. Induction of pluripotent stem cells from mouse embryonic and adult fibroblast cultures by defined factors. *Cell* **126**, 663-676, doi:10.1016/j.cell.2006.07.024 (2006).

36 Pampaloni, F., Reynaud, E. G. & Stelzer, E. H. The third dimension bridges the gap between cell culture and live tissue. *Nature reviews. Molecular cell biology* **8**, 839-845, doi:10.1038/nrm2236 (2007).

37 Astashkina, A. & Grainger, D. W. Critical analysis of 3-D organoid in vitro cell culture models for high-throughput drug candidate toxicity assessments. *Advanced drug delivery reviews* **69-70**, 1-18, doi:10.1016/j.addr.2014.02.008 (2014).

38 Carvalho, H. M., Teel, L. D., Goping, G. & O'Brien, A. D. A three-dimensional tissue culture model for the study of attach and efface lesion formation by enteropathogenic and enterohaemorrhagic Escherichia coli. *Cellular microbiology* **7**, 1771-1781, doi:10.1111/j.1462-5822.2004.00594.x (2005).

39 Nickerson, C. A., Goodwin, T. J., Terlonge, J., Ott, C. M., Buchanan, K. L., Uicker, W. C., Emami, K., LeBlanc, C. L., Ramamurthy, R., Clarke, M. S., Vanderburg, C. R., Hammond, T. & Pierson, D. L. Three-dimensional tissue assemblies: novel models for the study of Salmonella enterica serovar Typhimurium pathogenesis. *Infection and immunity* **69**, 7106-7120, doi:10.1128/IAI.69.11.7106-7120.2001 (2001).

40 Honer zu Bentrup, K., Ramamurthy, R., Ott, C. M., Emami, K., Nelman-Gonzalez, M., Wilson, J. W., Richter, E. G., Goodwin, T. J., Alexander, J. S., Pierson, D. L., Pellis, N., Buchanan, K. L. & Nickerson, C. A. Three-dimensional organotypic models of human colonic epithelium to study the early stages of enteric salmonellosis. *Microbes and infection / Institut Pasteur* **8**, 1813-1825, doi:10.1016/j.micinf.2006.02.020 (2006).

41 Carterson, A. J., Honer zu Bentrup, K., Ott, C. M., Clarke, M. S., Pierson, D. L., Vanderburg, C. R., Buchanan, K. L., Nickerson, C. A. & Schurr, M. J. A549 lung epithelial cells grown as three-dimensional aggregates: alternative tissue culture

model for Pseudomonas aeruginosa pathogenesis. *Infection and immunity* **73**, 1129-1140, doi:10.1128/IAI.73.2.1129-1140.2005 (2005).

42 Smith, Y. C., Grande, K. K., Rasmussen, S. B. & O'Brien, A. D. Novel three-dimensional organoid model for evaluation of the interaction of uropathogenic Escherichia coli with terminally differentiated human urothelial cells. *Infection and immunity* **74**, 750-757, doi:10.1128/IAI.74.1.750-757.2006 (2006).

43 Banerjee, I., Fuseler, J. W., Price, R. L., Borg, T. K. & Baudino, T. A. Determination of cell types and numbers during cardiac development in the neonatal and adult rat and mouse. *American journal of physiology. Heart and circulatory physiology* **293**, H1883-1891, doi:10.1152/ajpheart.00514.2007 (2007).

44 Jugdutt, B. I. Remodeling of the myocardium and potential targets in the collagen degradation and synthesis pathways. *Current drug targets. Cardiovascular & haematological disorders* **3**, 1-30 (2003).

45 Kohl, P., Camelliti, P., Burton, F. L. & Smith, G. L. Electrical coupling of fibroblasts and myocytes: relevance for cardiac propagation. *Journal of electrocardiology* **38**, 45-50, doi:10.1016/j.jelectrocard.2005.06.096 (2005).

46 Camelliti, P., Borg, T. K. & Kohl, P. Structural and functional characterisation of cardiac fibroblasts. *Cardiovascular research* **65**, 40-51, doi:10.1016/j.cardiores.2004.08.020 (2005).

47 Imanishi, R., Ashizawa, N., Ohtsuru, A., Seto, S., Akiyama-Uchida, Y., Kawano, H., Kuroda, H., Nakashima, M., Saenko, V. A., Yamashita, S. & Yano, K. GH suppresses TGF-beta-mediated fibrosis and retains cardiac diastolic function. *Molecular and cellular endocrinology* **218**, 137-146, doi:10.1016/j.mce.2003.12.004 (2004).

48 Carrier, R. L., Papadaki, M., Rupnick, M., Schoen, F. J., Bursac, N., Langer, R., Freed, L. E. & Vunjak-Novakovic, G. Cardiac tissue engineering: cell seeding, cultivation parameters, and tissue construct characterization. *Biotechnology and bioengineering* **64**, 580-589 (1999).

49 Hosseinkhani, H., Hosseinkhani, M., Hattori, S., Matsuoka, R. & Kawaguchi, N. Micro and nano-scale in vitro 3D culture system for cardiac stem cells. *Journal of biomedical materials research. Part A* **94**, 1-8, doi:10.1002/jbm.a.32676 (2010).

50 Xie, Y., Hardouin, P., Zhu, Z., Tang, T., Dai, K. & Lu, J. Three-dimensional flow perfusion culture system for stem cell proliferation inside the critical-size beta-tricalcium phosphate scaffold. *Tissue engineering* **12**, 3535-3543, doi:10.1089/ten.2006.12.3535 (2006).

51 Zhao, F., Pathi, P., Grayson, W., Xing, Q., Locke, B. R. & Ma, T. Effects of oxygen transport on 3-d human mesenchymal stem cell metabolic activity in perfusion and static cultures: experiments and mathematical model. *Biotechnology progress* **21**, 1269-1280, doi:10.1021/bp0500664 (2005).

52 Volkmer, E., Drosse, I., Otto, S., Stangelmayer, A., Stengele, M., Kallukalam, B. C., Mutschler, W. & Schieker, M. Hypoxia in static and dynamic 3D culture systems for tissue engineering of bone. *Tissue engineering. Part A* **14**, 1331-1340, doi:10.1089/ten.tea.2007.0231 (2008).

53 Bancroft, G. N., Sikavitsas, V. I., van den Dolder, J., Sheffield, T. L., Ambrose, C. G., Jansen, J. A. & Mikos, A. G. Fluid flow increases mineralized matrix deposition in 3D perfusion culture of marrow stromal osteoblasts in a dose-dependent manner. *Proceedings of the National Academy of Sciences of the United States of America* **99**, 12600-12605, doi:10.1073/pnas.202296599 (2002).

54 Cheah, L. T., Dou, Y. H., Seymour, A. M., Dyer, C. E., Haswell, S. J., Wadhawan, J. D. & Greenman, J. Microfluidic perfusion system for maintaining viable heart tissue with real-time electrochemical monitoring of reactive oxygen species. *Lab on a chip* **10**, 2720-2726, doi:10.1039/c004910g (2010).

55 Cheah, L. T., Fritsch, I., Haswell, S. J. & Greenman, J. Evaluation of heart tissue viability under redox-magnetohydrodynamics conditions: toward fine-tuning flow in biological microfluidics applications. *Biotechnology and bioengineering* **109**, 1827-1834, doi:10.1002/bit.24426 (2012).

56 Liu, M. C., Shih, H. C., Wu, J. G., Weng, T. W., Wu, C. Y., Lu, J. C. & Tung, Y. C. Electrofluidic pressure sensor embedded microfluidic device: a study of endothelial cells under hydrostatic pressure and shear stress combinations. *Lab on a chip* **13**, 1743-1753, doi:10.1039/c3lc41414k (2013).

57 Shin, M., Matsuda, K., Ishii, O., Terai, H., Kaazempur-Mofrad, M., Borenstein, J., Detmar, M. & Vacanti, J. P. Endothelialized networks with a vascular geometry in microfabricated poly(dimethyl siloxane). *Biomedical microdevices* **6**, 269-278, doi:10.1023/B:BMMD.0000048559.29932.27 (2004).

58 van der Meer, A. D., Orlova, V. V., ten Dijke, P., van den Berg, A. & Mummery, C. L. Three-dimensional co-cultures of human endothelial cells and embryonic stem cell-derived pericytes inside a microfluidic device. *Lab on a chip* **13**, 3562-3568, doi:10.1039/c3lc50435b (2013).

59 You, L., Temiyasathit, S., Lee, P., Kim, C. H., Tummala, P., Yao, W., Kingery, W., Malone, A. M., Kwon, R. Y. & Jacobs, C. R. Osteocytes as mechanosensors in the inhibition of bone resorption due to mechanical loading. *Bone* **42**, 172-179, doi:10.1016/j.bone.2007.09.047 (2008).

60 Park, S. H., Sim, W. Y., Min, B. H., Yang, S. S., Khademhosseini, A. & Kaplan, D. L. Chip-based comparison of the osteogenesis of human bone marrow- and adipose tissue-derived mesenchymal stem cells under mechanical stimulation. *PloS one* **7**, e46689, doi:10.1371/journal.pone.0046689 (2012).

61 Torisawa, Y. S., Spina, C. S., Mammoto, T., Mammoto, A., Weaver, J. C., Tat, T., Collins, J. J. & Ingber, D. E. Bone marrow-on-a-chip replicates hematopoietic niche physiology in vitro. *Nature methods* **11**, 663-669, doi:10.1038/nmeth.2938 (2014).

62 Zhang, W., Lee, W. Y., Siegel, D. S., Tolias, P. & Zilberberg, J. Patient-specific 3D microfluidic tissue model for multiple myeloma. *Tissue engineering. Part C, Methods* **20**, 663-670, doi:10.1089/ten.TEC.2013.0490 (2014).

63 Zhang, Y., Gazit, Z., Pelled, G., Gazit, D. & Vunjak-Novakovic, G. Patterning osteogenesis by inducible gene expression in microfluidic culture systems. *Integrative biology : quantitative biosciences from nano to macro* **3**, 39-47, doi:10.1039/c0ib00053a (2011).

64 Park, J., Koito, H., Li, J. & Han, A. Microfluidic compartmentalized co-culture platform for CNS axon myelination research. *Biomedical microdevices* **11**, 1145-1153, doi:10.1007/s10544-009-9331-7 (2009).

65 Achyuta, A. K., Conway, A. J., Crouse, R. B., Bannister, E. C., Lee, R. N., Katnik, C. P., Behensky, A. A., Cuevas, J. & Sundaram, S. S. A modular approach to create a neurovascular unit-on-a-chip. *Lab on a chip* **13**, 542-553, doi:10.1039/c2lc41033h (2013).

66 Booth, R. & Kim, H. Characterization of a microfluidic in vitro model of the blood-brain barrier (muBBB). *Lab on a chip* **12**, 1784-1792, doi:10.1039/c2lc40094d (2012).

67 Griep, L. M., Wolbers, F., de Wagenaar, B., ter Braak, P. M., Weksler, B. B., Romero, I. A., Couraud, P. O., Vermes, I., van der Meer, A. D. & van den Berg, A. BBB on chip: microfluidic platform to mechanically and biochemically modulate blood-brain barrier function. *Biomedical microdevices* **15**, 145-150, doi:10.1007/s10544-012-9699-7 (2013).

68 Shayan, G., Choi, Y. S., Shusta, E. V., Shuler, M. L. & Lee, K. H. Murine in vitro model of the blood-brain barrier for evaluating drug transport. *European journal of pharmaceutical sciences : official journal of the European Federation for Pharmaceutical Sciences* **42**, 148-155, doi:10.1016/j.ejps.2010.11.005 (2011).

69 Shayan, G., Shuler, M. L. & Lee, K. H. The effect of astrocytes on the induction of barrier properties in aortic endothelial cells. *Biotechnology progress* **27**, 1137-1145, doi:10.1002/btpr.620 (2011).

70 Sung, K. E., Yang, N., Pehlke, C., Keely, P. J., Eliceiri, K. W., Friedl, A. & Beebe, D. J. Transition to invasion in breast cancer: a microfluidic in vitro model enables examination of spatial and temporal effects. *Integrative biology : quantitative biosciences from nano to macro* **3**, 439-450, doi:10.1039/c0ib00063a (2011).

71 Song, J. W., Cavnar, S. P., Walker, A. C., Luker, K. E., Gupta, M., Tung, Y. C., Luker, G. D. & Takayama, S. Microfluidic endothelium for studying the intravascular adhesion of metastatic breast cancer cells. *PloS one* **4**, e5756, doi:10.1371/journal.pone.0005756 (2009).

72 Chung, S., Sudo, R., Mack, P. J., Wan, C. R., Vickerman, V. & Kamm, R. D. Cell migration into scaffolds under co-culture conditions in a microfluidic platform. *Lab on a chip* **9**, 269-275, doi:10.1039/b807585a (2009).

73 Puleo, C. M., McIntosh Ambrose, W., Takezawa, T., Elisseeff, J. & Wang, T. H. Integration and application of vitrified collagen in multilayered microfluidic devices for corneal microtissue culture. *Lab on a chip* **9**, 3221-3227, doi:10.1039/b908332d (2009).

74 Imura, Y., Asano, Y., Sato, K. & Yoshimura, E. A microfluidic system to evaluate intestinal absorption. *Analytical sciences : the international journal of the Japan Society for Analytical Chemistry* **25**, 1403-1407 (2009).

75 Kimura, H., Yamamoto, T., Sakai, H., Sakai, Y. & Fujii, T. An integrated microfluidic system for long-term perfusion culture and on-line monitoring of intestinal tissue models. *Lab on a chip* **8**, 741-746, doi:10.1039/b717091b (2008).

76 Kim, H. J., Huh, D., Hamilton, G. & Ingber, D. E. Human gut-on-a-chip inhabited by microbial flora that experiences intestinal peristalsis-like motions and flow. *Lab on a chip* **12**, 2165-2174, doi:10.1039/c2lc40074j (2012).

77 Kim, H. J. & Ingber, D. E. Gut-on-a-Chip microenvironment induces human intestinal cells to undergo villus differentiation. *Integrative biology : quantitative biosciences from nano to macro* **5**, 1130-1140, doi:10.1039/c3ib40126j (2013).

78 Esch, M. B., Sung, J. H., Yang, J., Yu, C., Yu, J., March, J. C. & Shuler, M. L. On chip porous polymer membranes for integration of gastrointestinal tract epithelium with microfluidic 'body-on-a-chip' devices. *Biomedical microdevices* **14**, 895-906, doi:10.1007/s10544-012-9669-0 (2012).

79 Mahler, G. J., Esch, M. B., Glahn, R. P. & Shuler, M. L. Characterization of a gastrointestinal tract microscale cell culture analog used to predict drug toxicity. *Biotechnology and bioengineering* **104**, 193-205, doi:10.1002/bit.22366 (2009).

80 Jang, K. J., Cho, H. S., Kang do, H., Bae, W. G., Kwon, T. H. & Suh, K. Y. Fluid-shear-stress-induced translocation of aquaporin-2 and reorganization of actin cytoskeleton in renal tubular epithelial cells. *Integrative biology : quantitative biosciences from nano to macro* **3**, 134-141, doi:10.1039/c0ib00018c (2011).

81 Jang, K. J. & Suh, K. Y. A multi-layer microfluidic device for efficient culture and analysis of renal tubular cells. *Lab on a chip* **10**, 36-42, doi:10.1039/b907515a (2010).

82 Jang, K. J., Mehr, A. P., Hamilton, G. A., McPartlin, L. A., Chung, S., Suh, K. Y. & Ingber, D. E. Human kidney proximal tubule-on-a-chip for drug transport and nephrotoxicity assessment. *Integrative biology : quantitative biosciences from nano to macro* **5**, 1119-1129, doi:10.1039/c3ib40049b (2013).

83 Baudoin, R., Griscom, L., Monge, M., Legallais, C. & Leclerc, E. Development of a renal microchip for in vitro distal tubule models. *Biotechnology progress* **23**, 1245-1253, doi:10.1021/bp0603513 (2007).

84 Snouber, L. C., Letourneur, F., Chafey, P., Broussard, C., Monge, M., Legallais, C. & Leclerc, E. Analysis of transcriptomic and proteomic profiles demonstrates improved Madin-Darby canine kidney cell function in a renal microfluidic biochip. *Biotechnology progress* **28**, 474-484, doi:10.1002/btpr.743 (2012).

85 Carraro, A., Hsu, W. M., Kulig, K. M., Cheung, W. S., Miller, M. L., Weinberg, E. J., Swart, E. F., Kaazempur-Mofrad, M., Borenstein, J. T., Vacanti, J. P. & Neville, C. In vitro analysis of a hepatic device with intrinsic microvascular-based channels. *Biomedical microdevices* **10**, 795-805, doi:10.1007/s10544-008-9194-3 (2008).

86 Kane, B. J., Zinner, M. J., Yarmush, M. L. & Toner, M. Liver-specific functional studies in a microfluidic array of primary mammalian hepatocytes. *Analytical chemistry* **78**, 4291-4298, doi:10.1021/ac051856v (2006).

87 Lee, P. J., Hung, P. J. & Lee, L. P. An artificial liver sinusoid with a microfluidic endothelial-like barrier for primary hepatocyte culture. *Biotechnology and bioengineering* **97**, 1340-1346, doi:10.1002/bit.21360 (2007).

88 Nakao, Y., Kimura, H., Sakai, Y. & Fujii, T. Bile canaliculi formation by aligning rat primary hepatocytes in a microfluidic device. *Biomicrofluidics* **5**, 22212, doi:10.1063/1.3580753 (2011).

89 Sudo, R., Chung, S., Zervantonakis, I. K., Vickerman, V., Toshimitsu, Y., Griffith, L. G. & Kamm, R. D. Transport-mediated angiogenesis in 3D epithelial coculture. *FASEB journal : official publication of the Federation of American Societies for Experimental Biology* **23**, 2155-2164, doi:10.1096/fj.08-122820 (2009).

90 Allen, J. W., Khetani, S. R. & Bhatia, S. N. In vitro zonation and toxicity in a hepatocyte bioreactor. *Toxicological sciences : an official journal of the Society of Toxicology* **84**, 110-119, doi:10.1093/toxsci/kfi052 (2005).

91 Allen, J. W. & Bhatia, S. N. Formation of steady-state oxygen gradients in vitro: application to liver zonation. *Biotechnology and bioengineering* **82**, 253-262, doi:10.1002/bit.10569 (2003).

92 Chao, P., Maguire, T., Novik, E., Cheng, K. C. & Yarmush, M. L. Evaluation of a microfluidic based cell culture platform with primary human hepatocytes for the prediction of hepatic clearance in human. *Biochemical pharmacology* **78**, 625-632, doi:10.1016/j.bcp.2009.05.013 (2009).

93 Cheng, S., Prot, J. M., Leclerc, E. & Bois, F. Y. Zonation related function and ubiquitination regulation in human hepatocellular carcinoma cells in dynamic vs. static culture conditions. *BMC genomics* **13**, 54, doi:10.1186/1471-2164-13-54 (2012).

94 Legendre, A., Baudoin, R., Alberto, G., Paullier, P., Naudot, M., Bricks, T., Brocheton, J., Jacques, S., Cotton, J. & Leclerc, E. Metabolic characterization of primary rat hepatocytes cultivated in parallel microfluidic biochips. *Journal of pharmaceutical sciences* **102**, 3264-3276, doi:10.1002/jps.23466 (2013).

95 Sin, A., Chin, K. C., Jamil, M. F., Kostov, Y., Rao, G. & Shuler, M. L. The design and fabrication of three-chamber microscale cell culture analog devices with integrated dissolved oxygen sensors. *Biotechnology progress* **20**, 338-345, doi:10.1021/bp034077d (2004).

96 Sivaraman, A., Leach, J. K., Townsend, S., Iida, T., Hogan, B. J., Stolz, D. B., Fry, R., Samson, L. D., Tannenbaum, S. R. & Griffith, L. G. A microscale in vitro physiological model of the liver: predictive screens for drug metabolism and enzyme induction. *Current drug metabolism* **6**, 569-591 (2005).

97 Viravaidya, K. & Shuler, M. L. Incorporation of 3T3-L1 cells to mimic bioaccumulation in a microscale cell culture analog device for toxicity studies. *Biotechnology progress* **20**, 590-597, doi:10.1021/bp034238d (2004).

98 Toh, Y. C., Lim, T. C., Tai, D., Xiao, G., van Noort, D. & Yu, H. A microfluidic 3D hepatocyte chip for drug toxicity testing. *Lab on a chip* **9**, 2026-2035, doi:10.1039/b900912d (2009).

99 Novik, E., Maguire, T. J., Chao, P., Cheng, K. C. & Yarmush, M. L. A microfluidic hepatic coculture platform for cell-based drug metabolism studies. *Biochemical pharmacology* **79**, 1036-1044, doi:10.1016/j.bcp.2009.11.010 (2010).

100 Fritsche, C. S., Simsch, O., Weinberg, E. J., Orrick, B., Stamm, C., Kaazempur-Mofrad, M. R., Borenstein, J. T., Hetzer, R. & Vacanti, J. P. Pulmonary tissue engineering using dual-compartment polymer scaffolds with integrated vascular tree. *The International journal of artificial organs* **32**, 701-710 (2009).

101 Huh, D., Fujioka, H., Tung, Y. C., Futai, N., Paine, R., 3rd, Grotberg, J. B. & Takayama, S. Acoustically detectable cellular-level lung injury induced by fluid mechanical stresses in microfluidic airway systems. *Proceedings of the National Academy of Sciences of the United States of America* **104**, 18886-18891, doi:10.1073/pnas.0610868104 (2007).

102 Huh, D., Leslie, D. C., Matthews, B. D., Fraser, J. P., Jurek, S., Hamilton, G. A., Thorneloe, K. S., McAlexander, M. A. & Ingber, D. E. A human disease model of drug toxicity-induced pulmonary edema in a lung-on-a-chip microdevice. *Science translational medicine* **4**, 159ra147, doi:10.1126/scitranslmed.3004249 (2012).

103 Huh, D., Matthews, B. D., Mammoto, A., Montoya-Zavala, M., Hsin, H. Y. & Ingber, D. E. Reconstituting organ-level lung functions on a chip. *Science* **328**, 1662-1668, doi:10.1126/science.1188302 (2010).

104 Tavana, H., Zamankhan, P., Christensen, P. J., Grotberg, J. B. & Takayama, S. Epithelium damage and protection during reopening of occluded airways in a physiologic microfluidic pulmonary airway model. *Biomedical microdevices* **13**, 731-742, doi:10.1007/s10544-011-9543-5 (2011).

105 Grosberg, A., Nesmith, A. P., Goss, J. A., Brigham, M. D., McCain, M. L. & Parker, K. K. Muscle on a chip: in vitro contractility assays for smooth and striated muscle. *Journal of pharmacological and toxicological methods* **65**, 126-135, doi:10.1016/j.vascn.2012.04.001 (2012).

106 Xiao, R. R., Zeng, W. J., Li, Y. T., Zou, W., Wang, L., Pei, X. F., Xie, M. & Huang, W. H. Simultaneous generation of gradients with gradually changed slope in a microfluidic device for quantifying axon response. *Analytical chemistry* **85**, 7842-7850, doi:10.1021/ac4022055 (2013).

107 Tsantoulas, C., Farmer, C., Machado, P., Baba, K., McMahon, S. B. & Raouf, R. Probing functional properties of nociceptive axons using a microfluidic culture system. *PloS one* **8**, e80722, doi:10.1371/journal.pone.0080722 (2013).

108 Ziegler, L., Grigoryan, S., Yang, I. H., Thakor, N. V. & Goldstein, R. S. Efficient generation of schwann cells from human embryonic stem cell-derived neurospheres. *Stem cell reviews* **7**, 394-403, doi:10.1007/s12015-010-9198-2 (2011).

109 Shi, M., Majumdar, D., Gao, Y., Brewer, B. M., Goodwin, C. R., McLean, J. A., Li, D. & Webb, D. J. Glia co-culture with neurons in microfluidic platforms promotes the formation and stabilization of synaptic contacts. *Lab on a chip* **13**, 3008-3021, doi:10.1039/c3lc50249j (2013).

110 Park, H. S., Liu, S., McDonald, J., Thakor, N. & Yang, I. H. Neuromuscular junction in a microfluidic device. *Conference proceedings : ... Annual International Conference of the IEEE Engineering in Medicine and Biology Society. IEEE Engineering in Medicine and Biology Society. Annual Conference* **2013**, 2833-2835, doi:10.1109/EMBC.2013.6610130 (2013).

111 O'Neill, A. T., Monteiro-Riviere, N. A. & Walker, G. M. Characterization of microfluidic human epidermal keratinocyte culture. *Cytotechnology* **56**, 197-207, doi:10.1007/s10616-008-9149-9 (2008).

112 Nichol, J. W., Koshy, S. T., Bae, H., Hwang, C. M., Yamanlar, S. & Khademhosseini, A. Cell-laden microengineered gelatin methacrylate hydrogels. *Biomaterials* **31**, 5536-5544, doi:10.1016/j.biomaterials.2010.03.064 (2010).

113 Butler, J. P., Tolic-Norrelykke, I. M., Fabry, B. & Fredberg, J. J. Traction fields, moments, and strain energy that cells exert on their surroundings. *American journal of physiology. Cell physiology* **282**, C595-605, doi:10.1152/ajpcell.00270.2001 (2002).

114 Tseng, Q., Wang, I., Duchemin-Pelletier, E., Azioune, A., Carpi, N., Gao, J., Filhol, O., Piel, M., Thery, M. & Balland, M. A new micropatterning method of soft substrates reveals that different tumorigenic signals can promote or reduce cell contraction levels. *Lab on a chip* **11**, 2231-2240, doi:10.1039/c0lc00641f (2011).

115 Alonso-Latorre, B., Meili, R., Bastounis, E., Del Alamo, J. C., Firtel, R. & Lasheras, J. C. Distribution of traction forces associated with shape changes during amoeboid cell migration. *Conference proceedings : ... Annual International Conference of the IEEE Engineering in Medicine and Biology Society. IEEE Engineering in Medicine and Biology Society. Annual Conference* **2009**, 3346-3349, doi:10.1109/IEMBS.2009.5333191 (2009).

116 Furchgott, R. F. The receptors for epinephrine and norepinephrine (adrenergic receptors). *Pharmacological reviews* **11**, 429-441; discussion 441-422 (1959).

117 Warn-Cramer, B. J., Cottrell, G. T., Burt, J. M. & Lau, A. F. Regulation of connexin-43 gap junctional intercellular communication by mitogen-activated protein kinase. *The Journal of biological chemistry* **273**, 9188-9196 (1998).

118 Gaudesius, G., Miragoli, M., Thomas, S. P. & Rohr, S. Coupling of cardiac electrical activity over extended distances by fibroblasts of cardiac origin. *Circulation research* **93**, 421-428, doi:10.1161/01.RES.0000089258.40661.0C (2003).

119 Aung, A., Seo, Y. N., Lu, S., Wang, Y., Jamora, C., del Alamo, J. C. & Varghese, S. 3D traction stresses activate protease-dependent invasion of cancer cells. *Biophysical journal* **107**, 2528-2537, doi:10.1016/j.bpj.2014.07.078 (2014).

120 Ozeki, T., Kwon, M. H., Gu, J., Collins, M. J., Brassil, J. M., Miller, M. B., Jr., Gullapalli, R. P., Zhuo, J., Pierson, R. N., 3rd, Griffith, B. P. & Poston, R. S. Heart preservation using continuous ex vivo perfusion improves viability and functional recovery. *Circulation journal : official journal of the Japanese Circulation Society* **71**, 153-159 (2007).